The Diversity and Physiological Roles of NADH Dehydrogenase in Acetic Acid Bacteria

（酢酸菌における NADH デヒドロゲナーゼの多様性と生理学的役割）

PhD Thesis

Feronika Heppy Sriherfyna

A thesis submitted in partial fulfillment of the requirement for the degree of doctor of life science

Graduate School of Sciences and Technology for Innovation
Yamaguchi University
March, 2021

CONTENTS

Pages

LIST OF TABLES

Tables

Pages

CHAPTER 3

APPENDIX

LIST OF FIGURES

Figures

Pages

LIST OF ABBREVIATIONS

AAB	Acetic acid bacteria
ADP	Adenosine diphosphate
a-NDH	Auxiliary NADH dehydrogenase
ATP	Adenosine triphosphate
DDM	*n*-dodecyl-β-D-maltoside
DNA	Deoxyribonucleic acid
EMP	Embden-Mayerhof-Parnas pathway
EDP	Entner-Doudoroff pathway
GDH	Glucose dehydrogenase
gdhM	Membrane-bound glucose dehydrogenase
GLDH	Glycerol dehydrogenase
Gln	Glutamine
Glu	Glutamic acid
HGT	Horizontal gene transfer
HPLC	High-performance liquid chromatography
mRNA	Messenger ribonucleic acid
MTT	3-(4,5-dimethylthiazolyl-2)-2,5-diphenyltetrazolium bromide
NADH	Nicotinamide adenine dinucleotide
NADPH	Nicotinamide adenine dinucleotide phosphate
NDH	NADH dehydrogenase
NRC	Nitrate respiration chain
OD	Optical density
ORFs	Open reading frames
PCR	Polymerase chain reaction
PMF	Proton motive force
p-NDH	Primary NADH dehydrogenase
PPP	Pentose Phosphate Pathway
PQQ	Pyrroloquinoline quinone
Q1	Ubiquinone 1
RI	Refraction index

TCA	Tricarboxylic acid cycle
THase	Transhydrogenase
WT	Wild type
YPD	Yeast-peptone-glucose medium
YPGD	Yeast-peptone-glycerol-glucose medium
2KGA	2-keto-gluconic acid
5KGA	5-keto-gluconic acid

CHAPTER 1
General Introduction

The industrial workhorse acetic acid bacteria (AAB) are obligate aerobes producing vinegar prominently belonging to the class *Alphaproteobacteria*, family of *Acetobacteraceae* (Matsushita *et al*., 1994; Yamada, 2016). This class possesses 17 genera consist of *Acetobacter*, *Gluconobacter*, *Gluconacetobacter*, *Asaia*, *Komagataeibacter*, *Acidomonas*, *Kozakia*, *Swaminathania*, *Saccharibacter*, *Neoasaia*, *Granulibacter*, *Tanticharoenia*, *Ameyamaea*, *Endobacter*, *Nguyenibacter*, *Swingsia*, and *Neokomagataea* (Yamada, 2016). Among 17 genera, *Acetobacter* and *Gluconobacter* have a several obvious characteristic differences. *Gluconobacter* is considered being separated from *Acetobacter* as its common ancestor (Matsutani *et al*., 2011). *Acetobacter* has the capability to oxidize ethanol to acetic acid and subsequently oxidizing acetic acid to carbondioxide and water. *Gluconobacter* has a preference to oxidize D-glucose rather than ethanol. Mannitol also serves as a favorable growth media for *Gluconobacter* rather than *Acetobacter* (Yamada, 2016). Based on the availability of flagellation, *Acetobacter* and *Gluconobacter* has peritrichous and polar flagellation, respectively. Both *Acetobacter* and *Gluconobacter* produce 2-keto-D-gluconate, 5-keto-D-gluconate, and some strains of *Gluconobacter* also produce 2,5-diketo-D-gluconate (Matsushita *et al*., 2003; Kataoka *et al*., 2015; Sainz *et al*., 2016; Yamada, 2016).

Gluconobacter oxydans, one of the promising industrial bacteria belonging to *Acetobacteraceae* family is a gram negative, obligate aerobe, ellipsoidal to rod shaped, and chemoorganotrophic bacteria, exert oxygen as a terminal electron acceptor in respiratory chain. The term "oxydans" of *G. oxydans* species refer to Latin word, "*oxys*", which means "sharp, acidic," and "*dans*", "giving" (Muynck *et al*., 2007). Naturally, it is non-pathogenic bacteria and could be thrived in sugary niches like fruits and flowers, honeybees, cider, beer, and wine (Gupta *et al*., 2001). Higher substrates oxidation rate and low biomass of *Gluconobacter* engendered auspicious industrial bacteria. *Gluconobacter* strains utilize D-glucose, D-mannitol, D-fructose, and several alcohol as a substrate to produce D-gluconic acid, 2-ketogluconic acid, L-sorbose (vitamin C synthesis), dihydroxyacetone and also biosensor application (Matsushita *et al.,* 1994, Macauley *et al*., 2001, Deppenmeier *et al*., 2002, Gupta *et al*., 2001, Muynck *et al*., 2007). The capability of incomplete oxidation is a unique

characteristic of *G. oxydans* strains. Deficiency in several enzymes involved in Embden-Mayerhof-Parnas pathway (EMP) and tricarboxylic acid cycle (TCA cycle), such as phosphofructokinase, and succinate dehydrogenase, permits the implementation of pentose phosphate and Entner-Doudoroff pathway to generate the energy for the growth of *Gluconobacter* (Muynck *et al*., 2007).

Substrate metabolisms couple with energy generation involving the respiratory chain are crucial for microbial growth. The energy as adenosine triphosphate (ATP) is produced by means of two systems comprises substrate-level phosphorylation and oxidative phosphorylation, which are synthesized in the substrate catabolism and engendered by proton motive force (PMF), respectively. Energy triggered by PMF supports cell processes and biosynthesis (Neidhardt *et al*., 1990).

The essential enzyme that occupies a pivotal role in respiration chain is NADH dehydrogenase (NDH) divided into three types, including type I NADH dehydrogenase (Complex I or NDH-1), type II or alternative NADH dehydrogenase (NDH-2), and sodium pumping NADH dehydrogenase (Nqr), encoded by *nuo*, *ndh*, and *nqr* genes, respectively (Nantapong *et al*., 2005; Kerscher *et al*., 2007). Cava *et al*., 2004 revealed a new type of NADH dehydrogenase, NRC, type IV NADH dehydrogenase involving in nitrate respiration in the *Thermus thermophiles*, an extreme thermophile bacterium. In case of AAB, each genus or species bear diverse NADH dehydrogenase types. *Acetobacter aceti* has two type I NADH dehydrogenase and type II NADH dehydrogenase encoded by *nuo1*, *nuo2*, and *ndh* genes, respectively (Arai *et al*., 2016). Other species, for instance, *Corynebacterium glutamicum* and *Gluconobacter oxydans* 621H have NDH-2 merely without NDH-1, meanwhile *Gluconobacter oxydans* DSM3504 possess only NDH-2 with another additional NDH-2 (Nantapong *et al*., 2005; Mogi *et al*., 2009; Kostner *et al*., 2015). Prust *et al*., (2005) postulated that *G. oxydans* has a Complex I and cytochrome *c* oxidase (Complex IV) shortage. *G. oxydans* NBRC 3293 exploited in this study has two NDH-2, primary NDH (p-NDH) and auxiliary NDH (a-NDH), as in *G. oxydans* DSM 3504. Prior studies revealed the importance of the additional NDH of *G. oxydans* DSM 3504 in increasing the growth yield of *G. oxydans* ATCC 621H possessing merely sole NDH (Kostner *et al*., 2015). Therefore, in order to elucidate the diversity of the NADH dehydrogenase presences in AAB, the investigation of a gene repertoire analysis in entire procurable AAB genomes based on their phylogenetic relationship was conducted as a first work in this study.

As an obligate aerobe bacteria, NADH dehydrogenase of *G. oxydans* engaged in respiration chain catalyzing electron transfer from NAD(P)H to ubiquinone then oxygen as terminal electron acceptor. In generating energy for the growth, *G. oxydans* oxidize glucose in two ways, inside and outside the cell. $NADP^+$-dependent glucose dehydrogenase (GDH) acts to oxidize glucose inside the cell, whilst $NADP^+$-independent GDH has a part to enforce glucose oxidation outside the cell forming gluconic acid then subsequently metabolized via PPP. The latter mechanism also termed as "direct glucose oxidation" (Gupta *et al*., 2001). In addition, Krajewski *et al*., (2010) reported that elimination of membrane-bound glucose dehydrogenase (*gdhM*) enable to raise growth yields and growth rate of *G. oxydans* N44-1.

Lacking of NDHs information has been encouraged a second work and further investigation into biochemical properties of p-NDH and a-NDH in *G. oxydans* NBRC 3293. The utilization of *gdhM*-deficiency strain has not been executed as a host of *ndh* deletion gene. Hence, in this study, the construction of *G. oxydans* NBRC 3293 derivative defective in a-NDH was carried out in order to perceive the physiological role of a-NDH in *G. oxydans* strain.

CHAPTER 2

Diversity of NADH Dehydrogenase in Acetic Acid Bacteria: Adaptation to Modify Their Phenotype through Gene Expansions and Losses and Neo-functionalization

Abstract

NADH dehydrogenase plays an important role in the central metabolism of almost all organisms, including acetic acid bacteria (AAB). In this study, the gene diversity of the NADH dehydrogenases in AAB was investigated. The distribution of the genes of the type I and type II NADH dehydrogenases in AAB was mostly congruent with their phylogenetic relationships. There are two phylogenetically distinct type I NADH dehydrogenase complexes, complex IA and complex IE. Complex IA', which lacks the *nuoM* gene from complex IA, was only conserved in the genera *Acetobacter, Gluconacetobacter* and *Komagataeibacter*, which all have the ability to perform acetic acid fermentation, whereas the complex IE gene cluster was found randomly in several species of AAB. Almost all AAB, excluding the early-diverged species, had the type II NADH dehydrogenase, while some of the species also had the homologue with an amino acid replacement at the residue responsible for NADPH oxidation ability. Thus, the gene repertoire of NADH dehydrogenases shows a history of adaptation towards their habitats through gene expansions and losses and neo-functionalization in AAB.

2.1 Results and discussion

Acetic acid bacteria (AAB) are strictly aerobic α-proteobacteria that are known to have a strong ability to incompletely oxidize ethanol, sugars and sugar alcohols to produce the corresponding sugar acids. Two AAB genera, *Acetobacter* and *Komagataeibacter*, have traditionally been used for the industrial production of vinegar. These AAB exhibit ethanol oxidation to produce acetic acid in the first growth phase, and then acetic acid over-oxidation to assimilate acetic acid in the final growth phase in ethanol-containing medium (Kanchanarach *et al*., 2010). In the ethanol oxidation phase, the cells oxidize ethanol to acetic acid through the periplasmic oxidation system, which consists of a membrane-bound alcohol and aldehyde dehydrogenases and terminal ubiquinol oxidases in the respiratory chain (Matsushita *et al*., 1994). In the final over-oxidation phase, the cells assimilate the

acetic acid accumulated in the first growth phase via a modified TCA cycle (Mullins *et al*., 2008). By contrast, a species of another AAB genus, *Gluconobacter*, can oxidize a wide ranges of sugars, sugar acids, or sugar alcohols by a similar periplasmic oxidation system with several different membrane-bound dehydrogenases (Matsushita *et al*., 1994), but it cannot assimilate a large quantity of the oxidative products due to a defect in the TCA cycle (Bringer and Bott, 2016).

Membrane-bound NADH dehydrogenases play an important role in the central metabolism of these AAB. There are two types of membrane-bound NADH dehydrogenases: the type I enzymes that generate a proton-motive force and the type II non-generating enzymes (Matshushita *et al*., 1987). The type I proton-translocating NADH dehydrogenase (complex I) is a multi-subunit integral membrane enzyme, composed of 13 or 14 subunits, that is also found in eukaryotic organelles (Brandt, 2006). This complex is found in more than 50% of bacteria (Spero *et al*., 2015) and has been found to be separated phylogenetically into two distinct types of operon structures: complex I_A and complex I_E (Spero *et al*., 2016). Alternatively, the type II NADH dehydrogenase (Ndh) is encoded by a single gene and is also broadly distributed in a wide variety of bacteria, some archaea, and some Eukarya, especially in fungi; there are also some homologous proteins with amino acid substitutions (E/D to Q/N) in the substrate-binding site that are important for the discrimination of NADH and NADPH (Marreiros *et al*., 2016). Desplats *et al*. reported that the E203Q mutant of the type II NADH dehydrogenase from *Agrobacterium tumefaciens* is effective at oxidizing NADPH (Desplats *et al*., 2007). It has been shown from a comparison between two genomes of *Gluconobacter oxydans*, 621H and DSM3504, that there is an additional paralogous gene of the type II NADH dehydrogenase, which has the substrate-binding site residue E replaced with Q in the DSM3504 genome, and that the gene disruption of the paralogous Ndh causes a significant growth defect (Kostner *et al*., 2015). Furthermore, in another AAB species, *Acetobacter aceti*, it has been shown that there are two sets of complex I gene clusters in the genome, and one of the two complex I gene clusters shows higher expression in cells grown on acetic acid or glucose than in those grown on ethanol, probably because of the activation of the TCA cycle via NADH oxidation (Sakurai *et al*., 2011). Thus, these data suggest that there are several different NADH dehydrogenases in AAB and that some of them play critical roles in the physiology of AAB in some

specific growth phases.

Here, based on their phylogenetic relationships, a gene repertoire analysis of the NADH dehydrogenases in all available AAB genomes was performed. The analysis enabled us to elucidate a history of their adaptation to their habitats during evolution.

To retrieve amino acid sequence data, bacterial and archaeal genomes, selected as one genome per genus, which were categorized as reference and representative genomes, and 142 AAB genomes were downloaded from the NCBI Reference Sequence (RefSeq) database website at ftp.ncbi.nlm.nih.gov/ (Tatusova *et al*., 2014). A BLASTP search against all proteins encoded by the 142 AAB genomes was performed using the amino acid sequences of complex I and the type II enzymes (Ndh) from four AAB genomes: *Acetobacter pasteurianus* IFO 3191^T (GCA_000241625.1), *Acidiphilium cryptum* JF-5 (GCA_000016725.1), *Gluconacetobacter diazotrophicus* PAl 5^T (GCA_000021325.1) and *Komagataeibacter medellinensis* NBRC 3288^T (GCA_000182745.2) as a query. BLASTP searching using the dataset described above was performed with an E-value cut-off of 10^{-5} and a sequence overlap (query and subject) of ≥70% (Altschul *et al*., 1997). The amino acid sequences of complex I_A of IFO 3191^T, JF-5 and PAl 5^T; complex I_E of JF-5 and PAl 5^T; Ndh (E) of IFO 3191^T, JF-5 and PAl 5^T; and Ndh (E) of IFO 3191^T were used (see Table S2.1, available in the online version of this article). The resulting hits were collected and compared to each other based on the gene organization, sequence identity and phylogenetic relationship. The two types of complex I, complex I_A and complex I_E, were distinguished by the amino acid sequence identity and their operon structure, while the two types of the Ndh genes, Ndh (E) and Ndh (Q), were classified by the residue responsible for the activity on NADPH (Desplats *et al*., 2007).

For the phylogenetic analysis of each gene, BLASTP searching using the dataset described above was performed with an E-value cut-off of 10^{-5} and a sequence overlap (query and subject) of ≥70 %. The top 100 hits from each

homologous query – for example, the hits for NuoM of complex I_A and complex I_E, – were combined, and used for phylogenetic tree construction without duplicate hits (Altschul *et al*., 1997). A phylogenetic tree was constructed by the neighbour-joining method with 1000 bootstrap replicates using the MEGA 7.01 package (Kumar *et al*., 2016). For the genome-based phylogenetic approach, orthologous genes were identified and a genome-based phylogenetic tree of AAB species was constructed using a previously reported method (Matsutani *et al*., 2015). The 53 AAB genomes selected from each species, which were mainly composed of type strains, were defined as the reference AAB genome dataset and used for genome-based phylogenetic tree construction.

Many AAB have both type I and type II NADH dehydrogenases, complex I and Ndh respectively, which can be further separated into complex I_A and complex I_E and into Ndh (E) and Ndh (Q), based on having an E or Q amino acid residue in the substrate-binding site for NAD(P)H, respectively. Fig. 2.1 shows the organization of the genes related to complex I (*nuo* gene cluster) and Ndh (*ndh*) in the typical AAB, *Acetobacter pasteurianus* IFO 3191^T, and the early-diverged species, *Acidiphilium cryptum* JF-5. In *Acidiphilium*, there are two forms of complex I, complex I_A and complex I_E, where *nuoC* and *nuoD* are fused as *nuoC/D* in the complex I_E gene cluster (Spero *et al*., 2015). In *A. pasteurianus*, there is only complex I_A, for which the cluster has lost the *nuoM* gene that is encoded in another position, and is thus called complex I_A' to distinguish it from complex I_A of *A. cryptum*. *A. pasteurianus* also has two types of Ndh, Ndh (E) and Ndh (Q), besides complex I_A'. Therefore, these five groups, complex I_A, complex I_A', complex I_E, Ndh (E) and Ndh (Q), were examined for the 142 AAB genomes, and their distributions were compared.

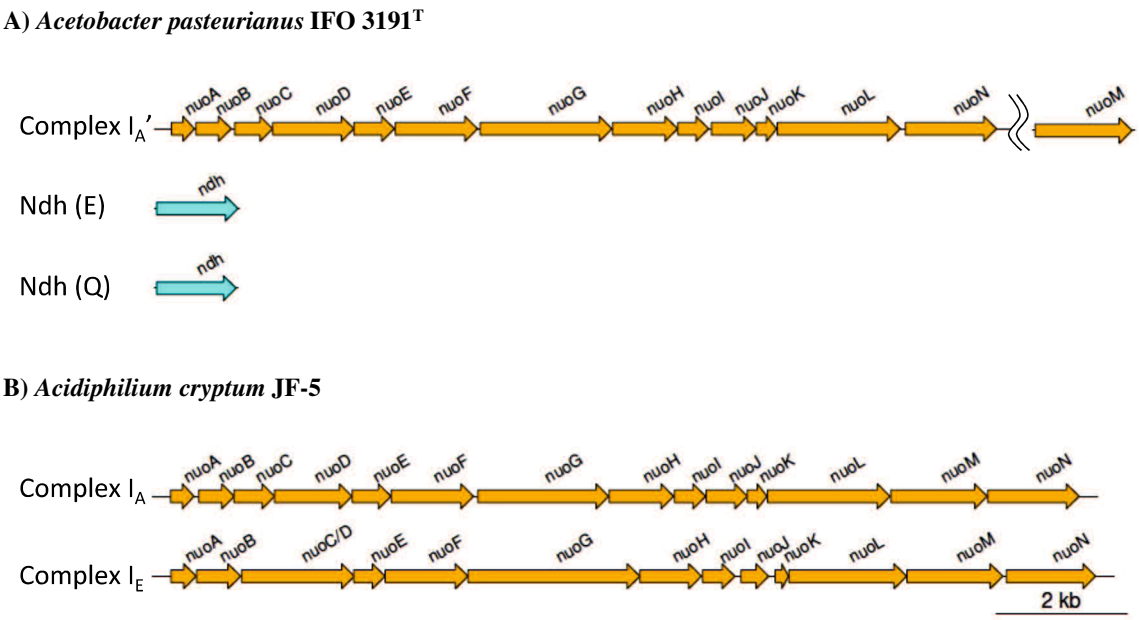

Fig. 2.1. Graphical representation of the NADH dehydrogenase gene clusters that are conserved in the AAB strain, (a) *Acetobacter pasteurianus* IFO 3191^T, and in the early-diverged strain, (b) *Acidiphilium cryptum* JF-5. The figure was drawn with genoPlotR (Guy *et al*., 2010). Orange and cyan arrows indicate the type I NADH dehydrogenase gene cluster (*nuo*) and type II NADH dehydrogenase gene (*ndh*), respectively.

To estimate their phylogenetic relationships, 53 reference genomes, selected from each AAB species, which were mainly composed of type strains of the 142 strains, were used (Fig. S2.1). The 53 strains were separated into 5 groups and 1 genus. Three genera, *Acidocella, Acidiphilium* and *Granulibacter*, were categorized as group E, which diverged from a common ancestor of AAB and this group (Fig. S1). The AAB genera were further divided into groups A, B, C, D and *Commensalibacter* (Fig. S2.1). Based on this phylogenetic relationship, the gene distribution of the five groups of the NADH dehydrogenase genes, complex I_A, complex I_A', complex I_E, Ndh (E) and Ndh (Q), was compared. Fig. 2.2 shows a graphical representation of the existence of each gene or gene cluster in AAB and their early-diverged groups. All of these genes from the 53 AAB genomes are also listed in Table S2.1. Members of phylogenetic group E have a complete complex I_A gene cluster (*nuoA* to *nuoN*) in their genome. Of these, only *Granulibacter* had an additional *nuoM* gene in another position of the genome sequence, besides that in the complete complex I_A cluster. Other AAB genera, *Commensalibacter, Acetobacter, Komagataeibacter* and

Gluconacetobacter, had complex I_A', which has the *nuoM* gene separate from the gene cluster that lacks the *nuoM* gene. This strongly suggests that the common ancestor of *Granulibacter* and the AAB (groups, A, B, C, D and *Commensalibacter*) acquired the *nuoM* gene, and the common ancestor of AAB lost the *nuoM* gene from the complex I_A gene cluster during evolution (Fig. 2.2). However, this complex I_A' was not found in any of the B, C, and D clades of AAB, indicating that a common ancestor of these clades lost the genes during the evolution process. Thus, it was shown that the gene distributions of complex I and Ndh are mostly congruent with their phylogenetic relationship.

It has been shown that the gene expression of the single *nuoM* gene and all other genes for complex I_A' are co-regulated in *A. aceti* (Sakurai *et al*., 2011), suggesting that the single *nuoM* gene and the 13 other genes, *nuoABCDEFGHIJKLN*, in the cluster are functioning together as complex I_A'. As these single *nuoM* genes are classified in the same clade as *nuoM* in the gene cluster for complex I_A' (Fig. S2.2), the single *nuoM* gene might have been acquired by a gene duplication or a horizontal gene transfer (HGT) event from a closely related genus. All other subunits of complex I_A and complex I_A' also showed a similar phylogenetic pattern (for an example, see *nuoF* in Fig. S2.3). For each subunit, the clade of complex I_E was phylogenetically distant from that of complex I_A (Figs S2.2 and S2.3). Complex I_A and I_A' could not be found in phylogenetic groups B, C, and D, meaning that the loss of this gene cluster occurred from a common ancestor of these three groups (Fig. 2.2). Sakurai *et al*. reported that this gene cluster (complex I_A') was highly expressed in *A. aceti* cells grown on acetic acid or glucose, compared with the cells grown on ethanol (Sakurai *et al*., 2011), and it has also been shown that the *nuoA2* gene, which is a part of complex I_A', is upregulated in the over-oxidation phase of *A. aceti* (Sakurai *et al*., 2012). Therefore, this gene cluster may be responsible for the over-oxidation phase of AAB. Indeed, AAB species with this gene cluster retain the modified TCA cycle that functions for the assimilation of acetic acid (Mullin *et al*., 2008).

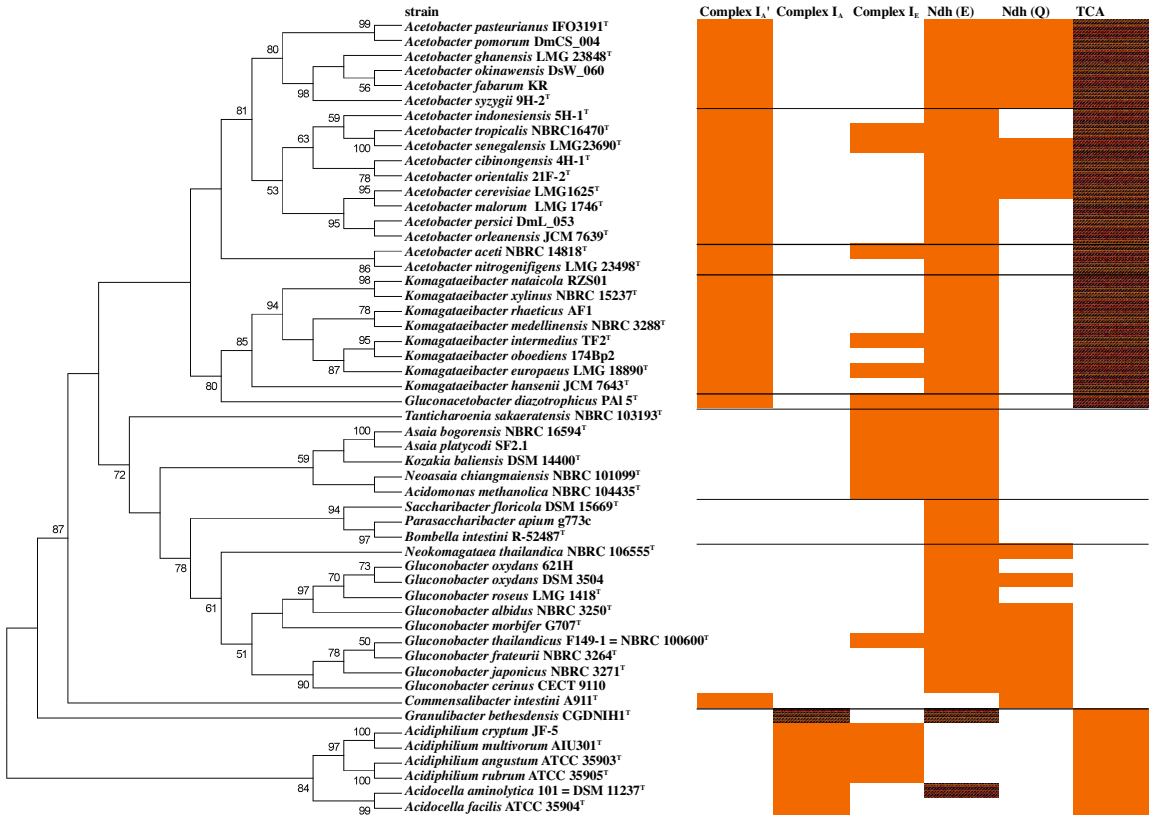

Fig. 2.2. Distribution of the NADH dehydrogenase genes: complex I_A, complex I_A', complex I_E, Ndh (E) and Ndh (Q), and the conservation of the TCA cycle in 53 AAB genomes. Dotted colours for complex I_A, Ndh (E) and TCA indicate the presence of an additional single *nuoM* gene, a phylogenetically distinct homologue and the modified TCA cycle with the *aarC* gene. The distribution is shown based on the phylogenetic relationship described in Fig. S2.1.

With the exception of the early-diverged species *Acidiphilium*, complex I_E is conserved in phylogenetic group B, all of the species of which only had complex I_E but not complex I_A', while some of the species that belong to phylogenetic group A, such as the genera *Acetobacter*, *Gluconacetobacter* and *Komagataeibacter*, had complex I_A'. However, these genes were not conserved at all in groups C and D (Fig. S2.1), which have do not have any complex I genes, except for *Gluconobacter thailandicus* (Fig. 2.2). As the ancestor of groups C and D seems to have lost complex I_E, *G. thailandicus* might have acquired the genes by an HGT event from other AAB species. It has also been reported that the stress-induced mutation (E183A) in the NuoF subunit of *Escherichia coli* permits the strain to have NADPH oxidation ability (Auriol *et al*., 2011), and we investigated the existence of such an amino acid

mutation using the 142 genomes. As a result, we found that two *Acidiphilium* and eight *Gluconobacter* strains had the same mutation that was responsible for the NADPH oxidation ability (Fig. S2.4). We summarized the gene gain and loss of each group (estimated evolutionary route) of type I NADH dehydrogenase genes in AAB (see Fig. S2.1). In this summary, we considered that the ancestor of all the reference strains retained both complex I_A and complex I_E.

Ndh (E) was conserved in all of the species of AAB that belong to phylogenetic groups A–D, while Ndh (Q) was only conserved in *Neokomagataea*, *Gluconobacter* and some *Acetobacter* species (see Figs. 2.2 and S2.1). Therefore, Ndh (E) may be an essential gene for AAB species. As described above, the gene-disrupted strain of Ndh (Q) showed significantly slower growth compared to the wild-type *G. oxydans* strain (Kostner *et al*., 2015). Therefore, not only Ndh (E), but also Ndh (Q), may play crucial roles for the growth of *Gluconobacter* species. Indeed, almost all *Gluconobacter* species retained Ndh (Q) (Table S2.2, available online at http://ds0n.cc.yamaguchi-u.ac.jp/~obi/sube.html). The phylogenetic analysis of the E and Q types of Ndh of AAB, together with Ndh from other taxonomic groups, indicated that both types of Ndh in AAB are classified in the same clade (Fig. S2.5). Therefore, it is suggested that the E/Q mutation could occur after the duplication of Ndh (E) in AAB species. Although Ndh (Q) was also conserved in *Commensalibacter*, this gene is phylogenetically distinct from the genes conserved in the other AAB genera.

As the incorrect assignment of species names makes it difficult to clarify differences in the gene repertoire in the same species, we reconstructed the whole genome-based phylogenetic relationship, including strains with a different gene repertoire than the reference strain. The results clearly indicated that the strains NBRC 101659, CECT 8443, 1023, 1.637, H24, WSH-003 and M-2 should be reclassified as appropriate species (Table S2.3 and Fig. S2.6). As a result, all *Gluconobacter* strains with the complex I_E gene cluster were classified as a single clade including the type strain of *G. thailandicus*. Therefore, this gene cluster may be useful as a molecular marker for strains belong to this clade (Fig. S2.6).

In summary, we have investigated the gene repertoire and the distribution of NADH dehydrogenases in AAB based on their whole genome-based phylogenetic

relationship. The results showed an evolutionary history of adaptation that had modified their phenotype through gene expansions and losses and neo-functionalization in AAB.

CHAPTER 3

The auxiliary NADH dehydrogenase plays a crucial role in redox homeostasis of nicotinamide cofactors in the absence of the periplasmic oxidation system in *Gluconobacter oxydans* NBRC3293

Abstract

Gluconobacter oxydans has the unique property of a glucose oxidation system in the periplasmic space, where glucose is oxidized incompletely to ketogluconic acids in a nicotinamide cofactor-independent manner. Elimination of the *gdhM* gene for membrane-bound glucose dehydrogenase, the first enzyme for the periplasmic glucose oxidation system, induces a metabolic change whereby glucose is oxidized in the cytoplasm to acetic acid. *G. oxydans* strain NBRC3293 possesses two molecular species of type II NADH dehydrogenase (NDH), the primary and auxiliary NDHs that oxidize NAD(P)H by reducing ubiquinone in the cell membrane. The substrate specificities of the two NDHs are different from each other: primary NDH (p-NDH) oxidizes NADH specifically but auxiliary NDH (a-NDH) oxidizes both NADH and NADPH. We constructed *G. oxydans* NBRC3293 derivatives defective in the *ndhA* gene for a-NDH, in the *gdhM* gene, and in both. Our Δ*gdhM* derivative yielded higher cell biomass on glucose, as reported previously, but grew at a lower rate than the wild-type strain. The Δ*ndhA* derivative showed growth behavior on glucose similar to that of the wild type. The Δ*gdhM* Δ*ndhA* double mutant showed greatly delayed growth on glucose, but its cell biomass was similar to that of the Δ*gdhM* strain. The double mutant accumulated intracellular levels of NAD(P)H and thus shifted the redox balance to reduction. Accumulated NAD(P)H levels might repress growth on glucose by limiting oxidative metabolisms in the cytoplasm. We suggest that a-NDH plays a crucial role in redox homeostasis of nicotinamide cofactors in the absence of the periplasmic oxidation system in *G. oxydans*.

Importance

Nicotinamide cofactors NAD^+ and $NADP^+$ mediate redox reactions in

metabolism. *Gluconobacter oxydans*, a member of the acetic acid bacteria, oxidizes glucose incompletely in the periplasmic space—outside the cell. This incomplete oxidation of glucose is independent of nicotinamide cofactors. However, if the periplasmic oxidation of glucose is abolished, the cells oxidize glucose in the cytoplasm by reducing nicotinamide cofactors. Reduced forms of nicotinamide cofactors are reoxidized by NADH dehydrogenase (NDH) on the cell membrane. We found that two kinds of NDH in *G. oxydans* have different substrate specificities: the primary enzyme is NADH specific, and the auxiliary one oxidizes both NADH and NADPH. Inactivation of the latter enzyme in *G. oxydans* cells in which we had induced cytoplasmic glucose oxidation resulted in elevated intracellular levels of NAD(P)H, limiting cell growth on glucose. We suggest that the auxiliary enzyme is important if *G. oxydans* grows independently of the periplasmic oxidation system.

3.1 Introduction

Gluconobacter oxydans is a Gram-negative bacterium belonging to the family *Acetobacteraceae*. It is an obligate aerobe that uses oxygen as a terminal electron acceptor in the respiratory chain. *Gluconobacter* spp. oxidize a wide variety of sugars, alcohols, and sugar alcohols to produce corresponding sugar acids, carboxylic acids, and sugars such as D-sorbitol, which is oxidized to L-sorbose for vitamin C synthesis. The ability to achieve incomplete oxidation is a major and unique characteristic of *Gluconobacter* spp. (Matsushita *et al*., 1994). A high oxidation rate of substances and low cell biomass are attractive features for an industrial microorganism. An incomplete Embden-Meyerhof-Parnas (EMP) pathway and tricarboxylic acid (TCA) cycle due to lack of the genes for phosphofructokinase and succinate dehydrogenase are the major metabolic features of this microorganism (Bringer and Bott, 2016). Glycolysis is dependent on the pentose phosphate pathway (PPP) and Entner-Doudoroff pathway (EDP) (Richhardt *et al*., 2013). Pyruvic acid is decarboxylated and oxidized; thus, acetic acid and carbon dioxide are the final metabolites (Peters *et al*., 2013).

Gluconobacter spp. oxidize glucose in the periplasmic space by using membrane- bound glucose dehydrogenase (GDH) to produce gluconic acid. Gluconic acid is subsequently oxidized by either PQQ-dependent, membrane-bound glycerol

dehydrogenase (GLDH) or flavoprotein gluconate dehydrogenase to produce 5-keto-gluconic acid (5KGA) or 2-keto-gluconic acid (2KGA), respectively (Fig. 3.1). 2KGA is further oxidized by 2KGA dehydrogenase to 2,5-diketo-gluconic acid in a few species of the family *Acetobacteraceae*, including *G. oxydans* strain NBRC3293 (Matsushita *et al*., 2003; Adachi *et al*., 2010; Kataoka *et al*., 2015; Adachi *et al*., 2016). In contrast to the cytoplasmic oxidation, the periplasmic oxidation is a unique feature of *Gluconobacter* spp. and other acetic acid bacteria (Matsushita *et al*., 1994). Glucose, gluconic acid, and ketogluconic acids may be imported into the cytoplasm, being metabolized via the PPP and EDP after appropriate redox reactions to produce acetic acid and carbon dioxide as the final metabolites (Fig. 3.1). However, typical growth behavior of *Gluconobacter* spp. produces gluconic and ketogluconic acids in a nearly stoichiometric amount, but the consumption of sugar acids seems to be repressed (Kataoka *et al*., 2015). Krajewski *et al*. (Krajewski *et al*., 2010) reported that elimination of the gene for GDH (*gdhM*) enabled the consumption of large amounts of glucose, leading to an increase in growth yield of *G. oxydans* strain N44-1. The elimination of *gdhM* somehow induces some metabolic changes not only in the periplasm but also in the cytoplasm. In this study, in order to gain insight into the metabolic change, we examined the glucose metabolism of *G. oxydans* strain NBRC3293, which is the parental strain of N44-1 (Sugisawa *et al*., 1990).

We anticipated that redox metabolism in the cytoplasm would be the key to understanding the effect of *gdhM* elimination, because a single oxidation step producing NADPH is increased if glucose rather than gluconate is imported into the cytoplasm (Adachi *et al*., 1979; Adachi *et al*., 1980) (Fig. 3.1). *G. oxydans* strain DSM3504 has the unique feature of possessing two genes for type II NADH dehydrogenase (NDH) (Kostner *et al*., 2015). NDH is a membrane-bound enzyme that catalyzes oxidation of NADH and reduces the membranous ubiquinone that connects the reducing equivalents to the electron transport chain, i.e., to molecular oxygen as the terminal electron acceptor. According to our bioinformatics study (Matsutani *et al*., 2019), most species of the family *Acetobacteraceae*, including *G. oxydans* strain ATCC 621H, possess the gene for a class of NDH; here, we refer to this class of NDH as primary NDH (p-NDH). On the other hand, a limited number of species and strains of the genera *Acetobacter* and *Gluconobacter* possess the gene for another class of NDH; we refer to this class of NDH as auxiliary NDH (a-NDH).

Importantly, the previous study showed that elimination of the gene for a-NDH (GLS_c05650) in *G. oxydans* DSM3504 partly inhibited its growth on mannitol (Kostner *et al*., 2015).

In this study, we determined the draft genome sequence of *G. oxydans* NBRC3293 to understand the gene repertoire related to the metabolism of glucose and nicotinamide cofactors. The metabolic features of *Gluconobacter* spp. seem to be conserved in the *G. oxydans* NBRC3293 genome, as the gene repertoire was more similar to that of DSM3504 than that of 621H, and the genes for p-NDH (*ndhP*) and a-NDH (*ndhA*) were found in the NBRC3293 genome. In this study, we constructed a *G. oxydans* NBRC3293 derivative that lacked both the *gdhM* and *ndhA* genes, in order to understand the impact of a-NDH on cytoplasmic glucose metabolism in the absence of the periplasmic glucose oxidation system. We found that a-NDH oxidizes both NADH and NADPH and maintains a low NAD(P)H/NAD(P)$^+$ redox ratio, particularly under GDH-deficient conditions.

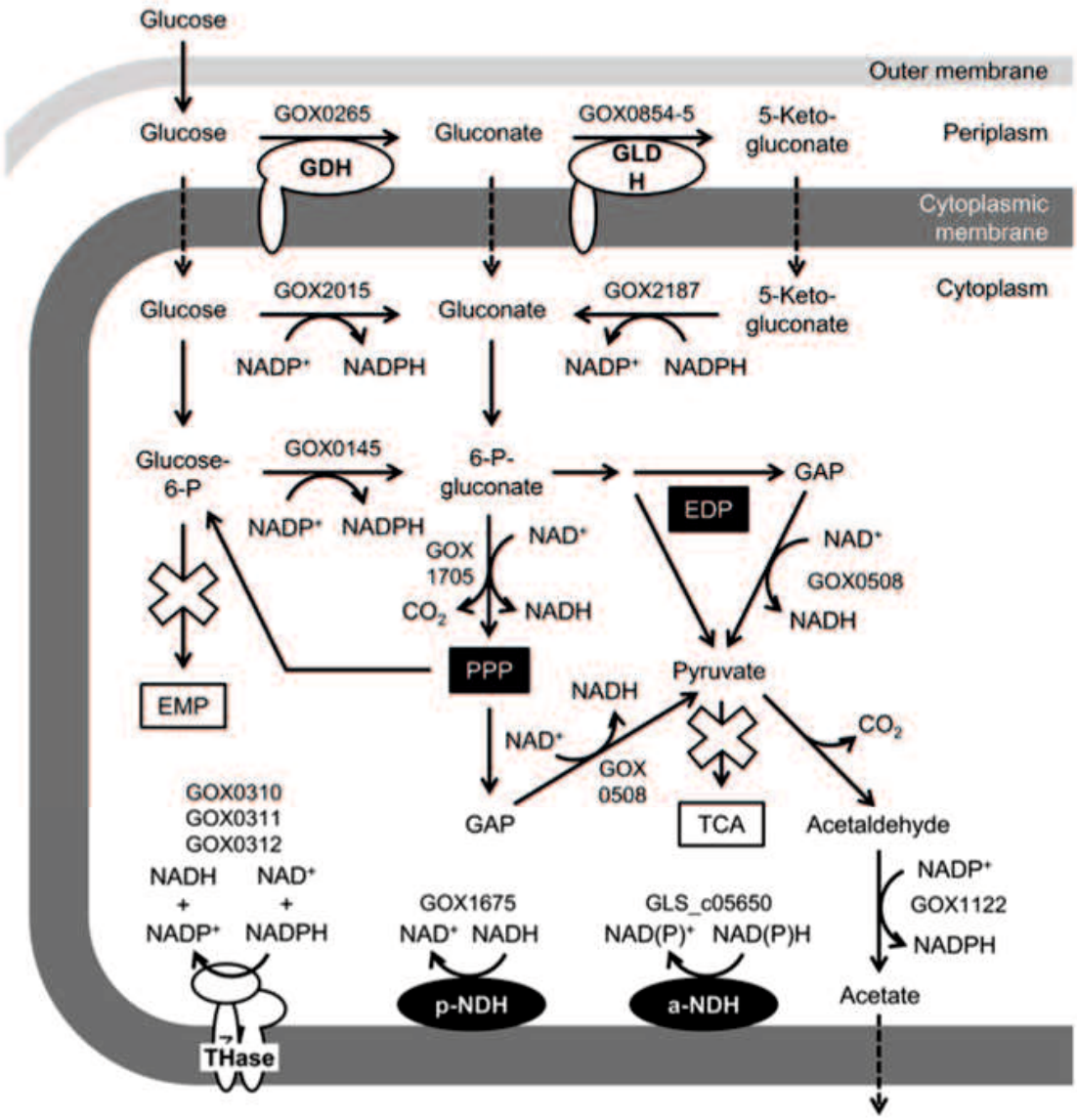

Fig. 3.1. Metabolism and nicotinamide cofactors in *Gluconobacter oxydans* on glucose. Redox reactions are shown with the locus tags for the genes of *G. oxydans* ATCC 621H, except for a-NDH, which is not found in the ATCC 621H genome. The locus tag of *G. oxydans* DSM3504 is used for a-NDH. Glucose is metabolized to acetic acid via the pentose phosphate pathway (PPP) or Entner-Doudoroff pathway (EDP) in *G. oxydans*. In the early stage of the glucose metabolism, only one route for the oxidation of gluconate and the reduction of 5-keto-gluconate is shown for simplicity. Another route not shown here is also possible via the membrane-bound gluconate 2-dehydrogenase (GOX1230-1232) and the 2-keto-gluconate reductase (GOX0417). GDH, membrane-bound glucose dehydrogenase; GLDH, membrane-bound glycerol dehydrogenase; EMP, Embden-Meyerhof-Parnas pathway; TCA, tricarboxylic acid cycle; GAP, glyceraldehyde-3-phosphate; THase, transhydrogenase; p-NDH, primary NADH dehydrogenase; a-NDH, auxiliary NADH dehydrogenase.

3.2 Results

3.2.1 Genome characteristics for whole-genome sequencing of *G. oxydans* NBRC3293

The genomic features of the NBRC3293 genome are shown in Table S3.1 in the supplemental material. Gene products were assigned to the KEGG metabolic pathway using the program GhostKOALA (Kanehisa *et al*., 2016). The assigned gene products were compared to those of other *G. oxydans* genomes, those of strains DSM3504 (Kostner *et al*., 2015) and ATCC 621H (Prust *et al*., 2005), but also to the genome of *Acetobacter pasteurianus* NBRC3283 (Azuma *et al*., 2009), a related strain in the family *Acetobacteraceae*, thereby elucidating the common and specific genes in NBRC3293 (Table S3.2, available online at http://ds0n.cc.yamaguchi-u.ac.jp/~obi/sube.html). The two type II NDHs, p-NDH and a-NDH, were conserved in NBRC3293 and had 99 and 100% amino acid sequence identities, respectively, to those from DSM3504. As previously reported for the *G. oxydans* 621H genome (Prust *et al*., 2005), NBRC3293 does not have the genes for phosphofructokinase and succinate dehydrogenase, making the EMP pathway and the tricarboxylic acid (TCA) cycle, respectively, incomplete. In contrast, genes for the EDP and the PPP are present in the NBRC3293 genome (Table S3.3).

3.2.2 Substrate specificities of p-NDH and a-NDH expressed in *Escherichia coli*

The plasmids for heterologous expression of p-NDH (NBRC3293_1744) and a-NDH (NBRC3293_0375) were constructed as described in Materials and Methods to transform the *E. coli* DKO strain, which lacks both type I and type II NDHs (Elguindy and Nakamaru-Ogiso, 2015). As shown in Table 3.1, the membranes of the recombinant *E. coli* strains harboring p-NDH were specific to NADH, whereas a-NDH oxidized both NADH and NADPH at similar rates.

Table 3.1. Properties of two NDHs expressed in *E. coli*[a]

NDH	NADH		NADPH	
	Sp act (U/mg)	**K_m (μM)**	**Sp act (U/mg)**	**K_m (μM)**
p-NDH	61.5 ± 12	147 ± 16	0.543 ± 0.11	253 ± 67
p-NDH-E189Q	5.92 ± 0.79	114 ± 17	3.95 ± 0.52	110 ± 16
a-NDH	15.1 ±1.4	348 ± 91	17.0 ± 1.5	35.1 ± 7.7
a-NDH-Q213E	12.4 ± 3.0	97.0 ± 30	1.34 ± 0.33	$>10^6$

[a]The membranes of the recombinant *E. coli* DKO strains that express *Gluconobacter* NDH as a sole NDH enzyme were used. NDH activity was measured by examining the decrease in absorbance at 340 nm in the presence of 60 μM Q1. Specific NDH activities were determined with 100 μM NAD(P)H. The K_m values for NAD(P)H were calculated on KaleidaGraph version 4.5 (Synergy Software, Reading, PA). See also Fig. S3.2.

The determinant for the substrate specificity in NDH has been proposed biochemically and structurally (Desplats *et al*., 2007; Heikal *et al*., 2014). As shown in Fig. S3.1, the Glu residue in *Agrobacterium tumefaciens* (currently *Agrobacterium fabrum*) NDH has been shown to be important for substrate specificity by biochemical analysis on the NDH derivatives with the amino acid replacement (Desplats *et al*., 2007). In addition, the 198th Glu residue in the crystal structure of *Caldalkalibacillus thermarum* NDH, which corresponds to the critical Glu residue in the *A. tumefaciens* enzyme, is predicted to be adjacent to the ribose in the adenosine portion of NADH (Heikal *et al*., 2014) (Fig. S3.1). There may be electrostatic repulsion between the carboxylic group of the Glu residue and the negative charge of the phosphate group on the ribose in NADPH, making the reactivity to NADPH lower. Based on amino acid alignment, p-NDH and a-NDH have the 189th Glu and 213th Gln residues in this position, respectively (Fig. S3.1).

To examine the role of these amino acid residues in the substrate specificities of the two NDHs, we constructed derivatives with amino acid replacements, i.e., p-NDH with an E189Q substitution and a-NDH with a Q213E substitution. The reactivity of p-NDH-E189Q to NADPH was comparable to that to NADH, while the rate of NADPH oxidation of a-NDH-Q213E was much lower than the rate of NADH oxidation (Table 3.1). The K_m values of the wild-type enzymes and the derivatives showed interesting behavior upon the amino acid substitutions. As for p-NDH, the K_m values even for NADPH were not dramatically changed upon the substitution. The K_m value of a-NDH for NADH decreased by more than one-third, and, more notably, that for NADPH was dramatically increased by the substitution (Table 3.1).

These results suggest that the 189th Glu in p-NDH and the 213th Gln in a-NDH have important roles in determining the substrate specificity of the two NDHs.

3.2.3 Construction of *G. oxydans* derivatives defective in a-NDH, which is responsible for NADPH oxidation

We successfully obtained *G. oxydans* NBRC 3293 derivatives defective in a-NDH: the Δ*ndhA* strain and the Δ*ndhA* Δ*gdhM* double mutant strain. However, we failed to construct a mutant defective in p-NDH. According to our procedure for constructing a mutant strain, the possibility to create the mutant or wild-type strain should theoretically be the same; e.g., we obtained 13 candidates possessing the wild-type *ndhA* allele and 10 candidates with the deletion allele from the wild-type strain. However, when we examined the genomic *ndhP* allele of the second recombinants as the candidates for the deletion mutant strain using PCR, all 21 candidates showed bands of a length corresponding to the wild-type *ndhP* allele. Thus, we tentatively concluded that *ndhP* is an essential gene in *G. oxydans* NBRC3293.

We determined NDH activity in the membranes of the *G. oxydans* derivatives. Coupling with oxidation of NADH, NDH transfers electrons to ubiquinone in the membrane. Then, the reduced form of ubiquinone is oxidized by ubiquinol oxidase by reducing molecular oxygen. Here, we refer to NDH activity dependent on natural ubiquinone present in the membrane as NADH oxidase (Fig. 3.2A). On the other hand, we supplemented ubiquinone 1 (Q1), an artificial ubiquinone analog, to avoid the ubiquinone being a rate-limiting factor. Here, we refer to NDH activity in the presence of Q1 as NADH dehydrogenase (Fig. 3.2B). The NADPH oxidase and dehydrogenase activities were decreased in the Δ*ndhA* and Δ*ndhA* Δ*gdhM* strains, while those of NADH showed similar values in all strains. The results indicate that a-NDH is responsible for NADPH oxidation. The oxidase activity works at a lower rate than the dehydrogenase activity, at 0.78 U/mg versus 4.6 U/mg, on NADH for the wild-type membranes, suggesting that reoxidation of ubiquinone is a rate-limiting step (Fig. 3.2).

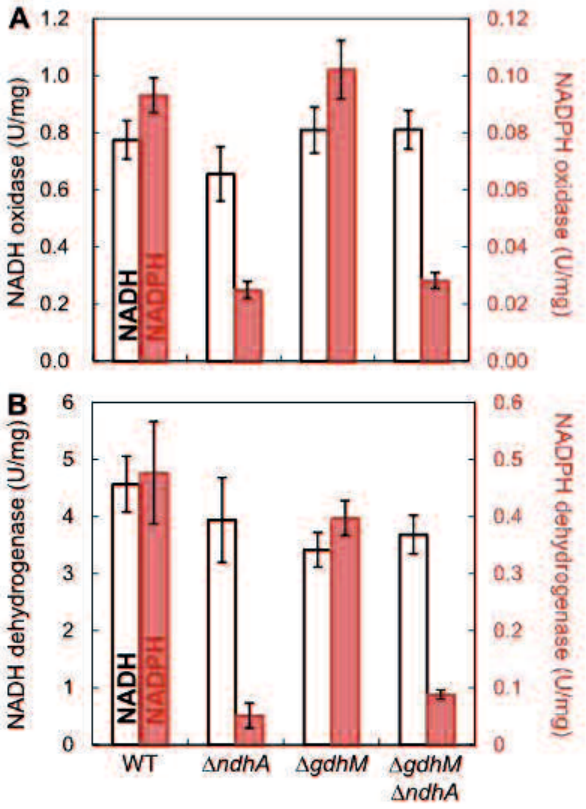

Fig. 3.2. Specific dehydrogenase and oxidase activities on NADH and NADPH in the membranes of the mutant strains of *Gluconobacter oxydans*. (A) NAD(P)H oxidase was measured by examining the decreases in absorbance at 340 nm in the absence of Q1. (B) NAD(P)H dehydrogenase was measured by examining the decreases in absorbance at 340 nm in the presence of 60 μM Q1. White bars, scaled by the left axis, and red bars, scaled by the right axis, indicate activities on NADH and NADPH, respectively. The mean values of triplicate experiments are shown, and the error bars represent the standard deviations. WT, wild type.

3.2.4 Elimination of the *ndhA* gene limits the growth on glucose of *G. oxydans* cells devoid of periplasmic oxidation

We examined the growth behavior of the *G. oxydans* derivatives on glucose. On glucose, the Δ*ndhA* strain grew as the wild type did, accompanied by similar glucose consumption and similar acetic acid production (Fig. 3.3). Rapid decreases in glucose and pH (Fig. S3.3) suggest gluconic acid production by GDH and further oxidation to ketogluconic and diketogluconic acids. Indeed, we qualitatively detected diketogluconic acid by high-performance liquid chromatography (HPLC) as the major metabolite in the medium of a 12-h culture (data not shown). The specific growth rate of Δ*ndhA* on glucose was nearly the same as that of the wild type (Table 3.2). On the

other hand, the cell yield of the Δ*gdhM* strain was more than twice that of the wild type as reported by Krajewski *et al.* (Krajewski *et al*., 2010). However, the specific growth rate on glucose of our Δ*gdhM* strain was lower than that of the wild type (Table 3.2), although the Δ*gdhM* derivative of the N44-1 strain grows faster than the parental strain (Krajewski *et al*., 2010). Glucose consumption in the Δ*gdhM* strain was slower than in the wild type due to the loss of GDH. In accordance with this, acetic acid was produced by the mutant strain with a much higher yield than the wild type (80% molar yield from 5 g/liter of glucose; 9.0% molar yield from 5 g/liter of glucose for the wild type). The Δ*gdhM* strain and also the Δ*ndhA* Δ*gdhM* strain produced negligible amounts of gluconic, ketogluconic, and diketogluconic acids (data not shown).

The double mutant Δ*ndhA* Δ*gdhM* strain showed a cell yield similar to that of the Δ*gdhM* strain on glucose (Fig. 3.3) but grew much more slowly than the Δ*gdhM* strain, of which the specific growth rate was nearly half that of the Δ*gdhM* strain (Table 3.2). The glucose consumption and acetic acid production of the double mutant strain were also slower than those of the Δ*gdhM* strain. Yields of acetic acid in the double mutant strain were much higher than in the wild type but a little lower than in the Δ*gdhM* strain (72% molar yield from 5 g/liter glucose).

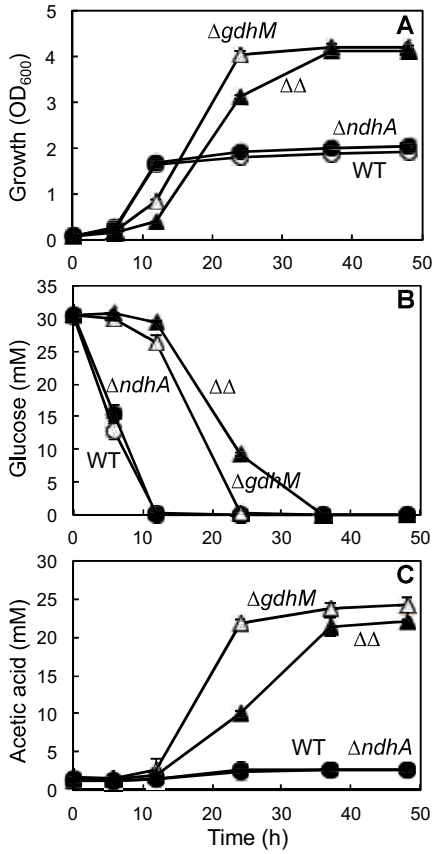

Fig. 3.3. Cultivation of the *G. oxydans* derivatives on glucose. The *G. oxydans* cells were cultivated on YPD medium using a 500-ml flask under shaking at 200 rpm. The mean values of triplicate cultivation for OD_{600} of growth (A), acetic acid (B), and glucose (C) were plotted, and the error bars represent the standard deviations. White circles, wild type (WT); black circles, Δ*ndhA*; white triangles, Δ*gdhM*; black triangles, Δ*gdhM* Δ*ndhA* (ΔΔ).

Table 3.2. Growth rates of *G. oxydans* derivatives on glucose and mannitol

Strain	Specific growth rate (h^{-1})[a]	
	Glucose	Mannitol
Wild type	61.5 ± 12	147 ± 16
Δ *ndhA* strain	5.92 ± 0.79	114 ± 17
Δ *gdhM* strain	15.1 ±1.4	348 ± 91
Δ *gdhM* Δ *ndhA* strain	12.4 ± 3.0	97.0 ± 30

[a]Specific growth rate was determined by measuring the OD_{600} of exponentially growing cells periodically. Mean values and standard deviations from the triplicate cultivations are shown.

3.2.5 Elimination of both the *ndhA* and *gdhM* genes increases the intracellular levels of the reduced forms of nicotinamide cofactors

We examined intracellular levels of NAD(P)H/NAD(P)$^+$ in the wild-type, Δ*ndhA*, Δ*gdhM*, and Δ*ndhA* Δ*gdhM* strains cultivated on glucose (Fig. 3.4), since NADPH oxidation activity in the membranes was decreased upon elimination of the *ndhA* gene (Fig. 3.2). The Δ*ndhA* strain had increased amounts of NADH and decreased amounts of NAD$^+$, making the NADH/NAD$^+$ ratio higher than in the wild type. In the case of NADPH/NADP$^+$, the amounts and the redox balance in Δ*ndhA* were similar to those in the wild type.

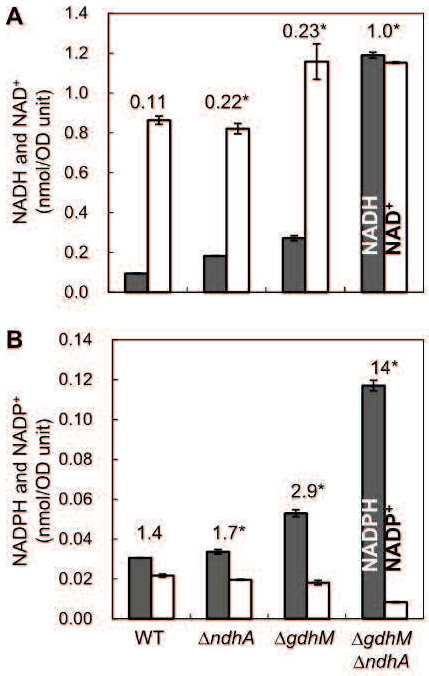

Fig. 3.4. Intracellular levels of NAD(P)H and NAD(P)$^+$ in the *G. oxydans* derivatives. The cells were grown on glucose and normalized by OD_{600}. (A) Gray and white bars indicate intracellular levels of NADH and NAD$^+$, respectively. The numbers above the bars indicate the NADH/NAD$^+$ ratios. (B) Gray and white bars indicate intracellular levels of NADPH and NADP$^+$, respectively. The numbers above the bars indicate the NADPH/NADP$^+$ ratios. The mean values of duplicate experiment are shown, and the error bars represent the standard deviations. We calculated *P* values for the difference in the NAD(P)H/NAD(P)$^+$ ratios between the wild type and each mutant strain. Asterisks indicate the *P* values less than 0.01.

The amounts of NADH and NADPH in the Δ*gdhM* strain were almost twice as high as that in the wild type, making the NAD(P)H/NAD(P)$^+$ ratio doubled. The Δ*ndhA* Δ*gdhM* double mutant strain showed considerably increased levels of both NADH and NADPH, with both the NADH/NAD$^+$ and NADPH/NADP$^+$ ratios

increased to 5 times those of the wild type.

G. oxydans NBRC3293 has the genes for transhydrogenase (THase), which transfers protons from NADPH to NAD^+, producing $NADP^+$ and NADH, coupled with pumping protons out across the membrane. It was reported that mRNA for THase is dramatically increased under oxygen-limited conditions in *G. oxydans* ATCC 621H (Hanke *et al*., 2012). Since we anticipate that THase may be involved in NAD(P)H redox homeostasis in our *G. oxydans* derivatives grown on glucose, we examined THase activity in the membranes. The *G. oxydans* strains showed THase activity of less than 0.02 U/mg, which was much lower than NDH activities (Fig. S3.4). Even if the activity was low, the THase action may account for the increased NADH levels in the Δ*gdhM* Δ*ndhA* double mutant, where THase might transfer hydrogen from highly accumulated NADPH to NAD^+, elevating NADH levels.

3.2.6 Elimination of the *ndhA* gene limits the second phase of growth of *G. oxydans* cells on mannitol

Previously it was reported that elimination of the *ndhA* (*GLS_c05650*) gene in the *G. oxydans* DSM3504 resulted in a reduced cell yield on mannitol (Kostner *et al*., 2015). Our Δ*ndhA* strain also showed a reduced cell yield on mannitol as reported (Fig. 3.5A). However, severe effects on growth rate were not observed, which was determined at the early stage of growth, when the cells grew exponentially: the values for optical density at 600 nm (OD_{600}) were less than 1.0 (Table 3.2). *G. oxydans* oxidizes mannitol to produce fructose and further oxidizes it to 5-ketofructose via the periplasmic polyol oxidation system (Ano *et al*., 2017), and then it consumes fructose and presumably 5-ketofructose (Fig. 3.5 and Fig. S3.5 and S3.6). The end metabolite of *G. oxydans* grown on mannitol is acetic acid (Richhardt *et al*., 2012). The Δ*ndhA* strain consumed fructose and 5-ketofructose slower than the wild-type strain (Fig. 3.5). Accordingly higher acetic acid productions were observed in the wild-type strain than the Δ*ndhA* strain (Fig. 3.5E). The Δ*gdhM* and double mutant Δ*ndhA* Δ*gdhM* strains showed growth behaviors similar to those of the wild-type and Δ*ndhA* strains, respectively (Fig. S3.6). The loss of a-NDH affected the second phase of growth presumably due to limited consumptions of fructose and 5-ketofructose, while the mutant cells grew as the wild type in the early stage of growth, when mannitol is

oxidized in the periplasm.

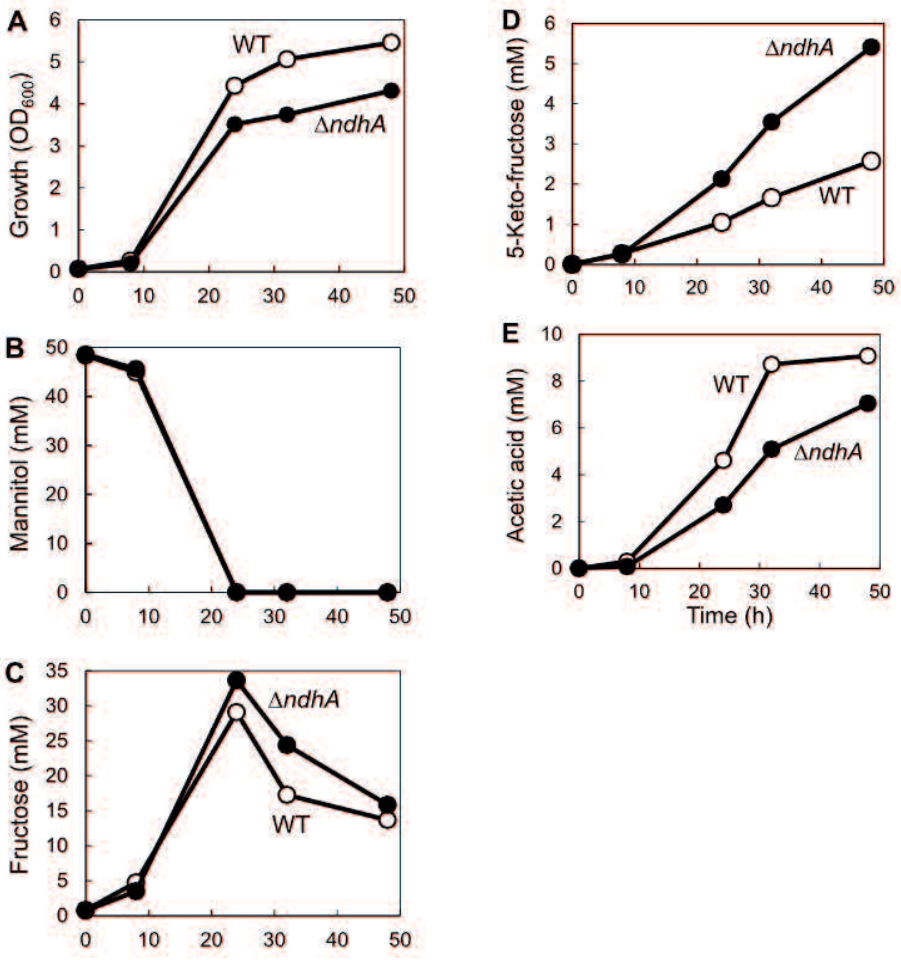

Fig. 3.5. Cultivation of the *G. oxydans* derivatives on mannitol. The *G. oxydans* cells were cultivated in mannitol medium with shaking at 200 rpm. The mean values of triplicate cultivation for OD_{600} of growth (A), mannitol (B), fructose (C), 5-ketofructose (D), and acetic acid (E) were plotted, and the error bars represent the standard deviations. White circles, WT; black circles, Δ*ndhA* strain.

3.3 Discussion

G. oxydans NBRC3293 possesses two type II NADH dehydrogenases, p-NDH and a-NDH, as mentioned above. Results obtained in this study indicate the functions of the two NDHs: p-NDH oxidizes NADH specifically, and a-NDH oxidizes both NADH and NADPH. In addition, expression levels of a-NDH seem to be much lower than those of p-NDH (Fig. 3.2). Amino acid replacements in the two NDHs suggested that the substrate specificities are largely determined by the amino acid residue which competes with phosphate group of NADPH, as has been previously suggested

(Desplats *et al*., 2007; Heikal *et al*., 2014; Marreiros *et al*., 2016).

Our Δ*gdhM* strain showed a lower specific growth rate on glucose than the wild-type strain. These results might account for an advantage of the GDH-dependent periplasmic glucose oxidation as for energy generation, i.e., proton motive force and ATP. However, since the reported Δ*gdhM* strain constructed from *G. oxydans* strain N44-1 strain grows faster than the parental strain (Krajewski *et al*., 2010), more careful validations of these results are required. Rather, other experimental setups, such as using an oxidation substrate that cannot be metabolized, may help to understand the impact of the periplasmic oxidation as for bioenergetics and cell growth. The N44-1 strain was developed from the NBRC3293 (formerly IFO3293) strain by the screening for 2-keto- L-gulonic acid production after repeated random mutagenesis (Sugisawa *et al*., 1990), suggesting the possible presence of some unidentified mutations in the genome. We suggest that not only the different growth conditions but also unidentified mutations in the N44-1 genome, if there were any, might account for the different growth behavior upon deletion of the *gdhM* gene.

The Δ*gdhM* Δ*ndhA* double mutant strain accumulated greatly reduced forms of nicotinamide cofactors compared to those of the corresponding single mutant strains (Fig. 3.4). If periplasmic oxidation is abolished, then the intracellular oxidative metabolic pathway is the only route for glucose metabolism to support cell growth. In this study, we deleted the gene for GDH to block the periplasmic oxidation of glucose, leading to metabolic change for glucose to the intracellular oxidation pathway, i.e., either $NADP^+$- dependent glucose dehydrogenase or $NADP^+$-dependent glucose-6-phosphate dehydrogenase (Fig. 3.1). Although both cases may produce much more NADPH than the wild type upon glucose metabolism, the single Δ*gdhM* mutation might affect the NADPH homeostasis only moderately because a-NDH would oxidize the NADPH produced. In the Δ*ndhA* strain, the NADPH levels would not be affected much, because there would be no additional NADPH production induced by the metabolic change. Indeed, the *G. oxydans* ATCC 621H strain is missing the gene for a-NDH naturally (Kostner *et* al., 2015; Matsutani *et* al., 2019). However, the double mutation Δ*gdhM* Δ*ndhA* consequently affects the NADPH/$NADP^+$ homeostasis severely, as NADPH in large amounts would not be oxidized in the absence of a-NDH (Fig. 3.4). The accumulated NADPH would jam oxidative metabolism of

glucose in the Δ*gdhM* Δ*ndhA* strain. We suggest that not only the NADPH oxidation system but also the periplasmic oxidation system are crucial for NADPH/$NADP^+$ homeostasis in *G. oxydans*. Increased levels of reduced forms of nicotinamide cofactors may inhibit oxidative metabolism using NAD^+ and $NADP^+$, affecting the cell growth.

The assumption mentioned above would be applicable to the cells grown on mannitol. In the early stage of growth, at which the cells oxidized mannitol in the periplasm, the Δ*ndhA* strain grew as well as the wild type (Fig. 3.5 and Table 3.2), which is similar to the case of cells grown on glucose (Fig. 3.3 and Table 3.2), suggesting that cell growth and therefore cytoplasmic metabolism tolerate the loss of a-NDH when the periplasmic oxidation system is operated. However, in the second phase of growth, at which the cells consumed fructose and 5-ketofructose, the Δ*ndhA* strain grew worse and consumed a smaller amount of sugars than the wild type (Fig. 3.5), suggesting that the loss of a-NDH jams cytoplasmic metabolism and therefore limits cell growth. The negative impact of the loss of a-NDH in the second phase of growth on mannitol could be observed in the cells growing on glucose with the Δ*gdhM* genetic background (Fig. 3.3 and Table 3.2).

The Δ*gdhM* Δ*ndhA* double mutant strain produced slightly less acetic acid than the Δ*gdhM* strain. Because the PPP produces less pyruvate than the EDP from one molecule of glucose, we suggest that the double mutant strain partially switched the metabolism to the PPP from the EDP. Carbon flux analysis on the wild-type *G. oxydans* ATCC 621H strain revealed that more than one-third of consumed glucose is metabolized via EDP in the early phase of growth but less than 10% in the late phase of growth (Hanke *et* al., 2013). However, it is not clear how the cells switch the metabolism and what is the physiological consequence of this metabolic change.

Incomplete oxidation via the periplasmic oxidation system is one of the key features of *Gluconobacter* spp., in which reoxidation of the reduced nicotinamide cofactors is not required, unlike the cytoplasmic oxidation reactions. We suggest that *Gluconobacter* spp. might have evolved the periplasmic oxidation system and thus independency of nicotinamide cofactors. When an aerobic organism additionally establishes a periplasmic oxidation system, oxidation of redox cofactors in the

cytoplasm might decline gradually generation by generation. Conversely, when a shortage of NAD(P)H oxidation limits cell growth, development of a periplasmic oxidation system would confer competitiveness. Therefore, when the metabolism of the nicotinamide cofactors was genetically modified in the cells which had induced cytoplasmic oxidation metabolism, the NADPH/$NADP^+$ ratio was dramatically elevated in *G. oxydans*. We suggest that this genetically modified *G. oxydans* strain could be applied as a laboratory tool for reductive biotransformations (Schweiger *et al*., 2010; Richter *et al*., 2009; Siedler *et al*., 2011). A combination of additional reductive metabolism mechanisms in our *G. oxydans* derivative may release the strain from the growth limitation observed in this study. This is under investigation.

3.4 Materials and Methods

3.4.1 Chemicals

NADH, NADPH, 3-acetylpyridine adenine dinucleotide, and yeast extract were supplied by Oriental Yeast (Tokyo, Japan). 5-Ketofructose was supplied by Kyowa-Hakko Bio (Tokyo, Japan). 5-Fluorocytosine was purchased from Fluorochem (Glossop, UK). Ubiquinone 1 [Q1; 2,3-dimethoxy-5-methyl-6-(3-methyl-2-butenyl)-1,4-benzoquinone] was supplied by Kimitoshi Sakamoto (Hirosaki University, Japan) (Sakamoto *et al*., 1996). The restriction enzymes and genetic manipulation reagents were obtained from Toyobo (Osaka, Japan). All other chemicals used in this study were commercial products.

3.4.2 Bacterial strains, plasmids, and culture conditions

The bacterial strains and plasmids used in this study are listed in Table 3.3. *Escherichia coli* strains were propagated at 30°C in modified Luria-Bertani (LB) medium composed of 5 g yeast extract, 10 g Hipolypepton (Nihon Pharmaceuticals, Osaka, Japan), and 5 g NaCl per liter, followed by pH adjustment at 7.0 with NaOH. When necessary, ampicillin and kanamycin were used at final concentrations of 50 μg ml^{-1} for *E. coli*. *G. oxydans* was cultivated at 30°C in ΔP medium (10 g yeast extract, 10 g Hipolypepton, 5 g glucose, and 20 g glycerol per liter), in mannitol medium (5 g yeast extract, 3 g Hipolypepton, and 9 g D-mannitol per liter, with pH adjustment to 6.0 with HCl) (Kostner *et al*., 2015), or in YPD medium (5 g yeast extract, 5 g

Hipolypepton, 6.8 g KH_2PO_4, and 5 g D-glucose per liter, with pH adjustment to 6.8 with KOH). When necessary, kanamycin was used at a final concentration of 100 μg ml^{-1} for *G. oxydans*.

The specific growth rate was determined by measuring the OD_{600} of exponentially growing cells periodically at 2- or 3-h intervals.

3.4.3 Genome sequencing, *de novo* assembly, and annotation

The genomic DNA of *G. oxydans* NBRC3293 was isolated by the method of Marmur (Marmur, 1961), with some modifications (Kawai *et al*., 2013). Illumina sequencing of the NBRC3293 strain was performed using the Illumina HiSeq 2000 sequencing platform with the paired-end strategy (2 × 100 bp) as previously described (Matsutani *et al*., 2014). Illumina sequence reads were assembled using Velvet version 1.2.07 (Zerbino and Birney, 2008). Protein-coding genes were predicted using Glimmer version 3.02 with a self-training data set (Salzberg *et al*., 1998; Delcher *et al*., 2007). Functional assignments of the predicted open reading frames (ORFs) were based on a BLASTP homology search against the NCBI nonredundant (NR) database (Altschul *et al*., 1997).

Table 3.3. Bacterial strains and plasmids used in this study

Strain or plasmid	Description	Source or reference(s)
Gluconobacter oxydans strains		
NBRC3293	Wild type	NBRC[a]
HK3	NBRC3293 Δ*gdhM*	This study
FHS1	NBRC3293 Δ*ndhA*	This study
FHS2	NBRC3293 Δ*gdhM* Δ*ndhA*	This study
Escherichia coli strains		
DH5α	Plasmid construction	Hanahan, 1983
HB101	Triparental mating	Boyer and Roulland-Dussoix, 1969
MC4100	F$^-$ *araD139* Δ(*argF-lac*)*U169 rpsL150 relA1 flbB5301 fruA25 deoC1 ptsF25*	Casadaban, 1976; Peters *et al*., 2003
DKO	MC4100 Δ*nuoB* (ΔNb1) Δ*ndh*::Spc^r	Elguindy and Nakamaru-Ogiso, 2015
Plasmids		
pBBR1MCS-4	Ap^r *mob codAB* P$_{lac}$; broad-host-range vector	Kovach *et al*., 1995
pTTQ18	Ap^r P$_{tac}$ *lacI*^{q}; expression vector for *E. coli*	Stark, 1987
pKOS6b	Km^r *mob codBA*; suicide vector for allelic exchange	Kostner *et al*., 2013
pK19*mobsacB*	Km^r *mob sacB*; suicide vector for allelic exchange	Schafer *et al*., 1994
pK19*mobsacB*Δ*gdhM*	pK19*mobsacB*, 1.0-kb Δ*gdhM* fragment	Krajewski *et al*., 2010
pFHS777	pBBR1MCS-4, 1.3-kb *ndhP* fragment	This study
pFHS785	pTTQ18, 1.3-kb *ndhP* fragment	This study
pES9	pTTQ18, 1.3-kb *ndhP* (E189Q) fragment	This study
pFHS779	pBBR1MCS-4, 1.4-kb *ndhA* fragment	This study
pFHS783	pTTQ18, 1.4-kb *ndhA* fragment	This study
pES8	pTTQ18, 1.4-kb *ndhA* (Q213E) fragment	This study
pHK2	pKOS6b, 1.0-kb Δ*gdhM* fragment	This study
pFHS11	pKOS6b, 1.2-kb Δ*ndhA* fragment	This study
pFHS12	pKOS6b, 1.5-kb Δ*ndhP* fragment	This study

[a]NBRC, Biological Resource Center, National Institute of Biotechnology and Evaluation (https://www.nite.go.jp/en/nbrc/).

3.4.4 Gene assignment to the KEGG metabolic map

Assignment of genes from NBRC3293 to the KEGG metabolic map was performed using GhostKOALA (Kanehisa *et al*., 2016). To search for undetected and disrupted genes in the draft genome assembly, a TBLASTN search against the NBRC3293 genome was performed. Amino acid sequences from *Acetobacter pasteurianus* IFO 3283-01 (GenBank accession numbers AP011121.1 to AP011127.1) were also used for the query sequence of the TBLASTN search for the

detection of genes absent in other *G. oxydans* strains (Altschul *et al*., 1997).

3.4.5 Plasmid construction

The gene for p-NDH (*NBRC3293_1744*; *ndhP*) was amplified from the genomic DNA of the *G. oxydans* NBRC3293 strain by Herculase DNA polymerase (Stratagene, La Jolla, CA) with the DNA primers ex-1744-5-Hin(+) and ex-1744-3-Xba(-). The purified 1.3-kb PCR product was digested with HindIII and XbaI and inserted into the corresponding site of pBBR1MCS-4 (Kovach *et al*., 1995) to construct pFHS777. Plasmid pFHS777 was treated with KpnI and XbaI to obtain a 1.3-kb DNA fragment containing the *ndhP* gene, followed by insertion into the corresponding site of pTTQ18 (Stark, 1987) to construct pFHS785. Substitution for the E189Q derivative was conducted using PfuUltra high-fidelity DNA polymerase (Stratagene) with the oligonucleotides 1744-E189Q(+) and 1744-E189Q(-), followed by digestion with DpnI. The plasmids for the gene encoding a-NDH (*NBRC3293_0375*; *ndhA*) were constructed with procedures similar to those for *ndhP*, but using the different oligonucleotides listed in Table 3.4.

Table 3.4. Oligonucleotides used in this study

Name	Sequence (5'-3')	Objective
ex-1744-5-Hin(+)	AAGCTTCGCACTTGATATGAGGAAAAATC	Expression of p-NDH
ex-1744-3-Xba(−)	TCTAGACGGGCTTCTGAAAAGGG	Expression of p-NDH
1744-E189Q(+)	GCTGAACGCCGTCCTGATCCAGACCGGCCCGCGCATCCTCC	E189Q substitution
1744-E189Q(−)	GGAGGATGCGCGGGCCGGTCTGGATCAGGACGGCGTTCAGC	E189Q substitution
ex-0375-5-Hin(+)	AAGCTTGCCCACCCCCTGAAC	Expression of a-NDH
ex-0375-3-Xba(−)	TCTAGAGTCCTTCATCGGGCTACAAG	Expression of a-NDH
0375-Q213E(+)	CTCCATGTCACGCTCCTGGAGTCCGGCGCGCGCATC	Q213E substitution
0375-Q213E(−)	GATGCGCGCGCCGGACTCCAGGAGCGTGACATGGAG	Q213E substitution
D-0375-5-Hin(+)	AAGCTTGGCACATCACGTTTATTTG	Deletion of *ndhA*
D-0375-fsn(+)	GCAGTACCGCCAATGATTTCTCCGACTGGGTCGAGACCTTC	Deletion of *ndhA*
D-0375-fsn(−)	GAAGGTCTCGACCCAGTCGGAGAAATCATTGGCGGTACTGC	Deletion of *ndhA*
D-0375-3-Xba(−)	TCTAGAAGGCGCTCCAGGTCTATTAC	Deletion of *ndhA*
D-1744-5-Kpn(+)	GGTACCGGACTGGCCGACAATC	Deletion of *ndhP*
D-1744-fsn(+)	GCTCGCGTGCGAATGACTTCACGGTCCGCGAACATCTTTC	Deletion of *ndhP*
D-1744-fsn(−)	GAAAGATGTTCGCGGACCGTGAAGTCATTCGCACGCGAGC	Deletion of *ndhP*
D-1744-3-Xba(−)	TCTAGAACCCAGTCCACGCCATC	Deletion of *ndhP*

To achieve deletion of the *gdhM* gene, which codes for the membrane-bound glucose dehydrogenase, a 1.0-kb DNA fragment containing a Δ*gdhM* allele was obtained by HindIII and XbaI digestion of plasmid pK19*mobsacB*Δ*gdhM* (Krajewski

et al., 2010), which was supplied by Stephanie Bringer and Michael Bott (Forschungszentrum Jülich, Germany). The DNA fragment containing a Δ*gdhM* allele was inserted into the HindIII and XbaI site of pKOS6b (Kostner *et al*., 2013) to construct pHK2.

In order to construct the deletion plasmid for the *ndhA* gene, a two-step PCR was conducted. The 5' and 3' regions of the *ndhA* gene were amplified from *G. oxydans* NBRC3293 genomic DNA by Herculase DNA polymerase with the following pairs of DNA primers: D-0375-5-Hin(+) and D-0375-fsn(-) for the 5' region and D-0375-fsn(+) and D-0375-3-Xba(-) for the 3' region. The PCR products were mixed, and the two DNA fragments were fused by DNA polymerase. The fused 1.2-kb DNA fragment was treated with HindIII and XbaI and inserted into the corresponding site of pKOS6b to construct pFHS11. Plasmid pFHS12 for deletion of the *ndhP* gene was constructed through two-step PCR as described above but using the different oligonucleotides listed in Table 3.4.

3.4.6 Deletion of the genes in *G. oxydans* NBRC3293

G. oxydans NBRC3293 was transformed with the targeted plasmid constructed as described above via a triparental mating method employing *E. coli* HB101/pRK2013 (Figurski and Helinski, 1979). Transformants were screened on YPGD agar medium (5 g D-glucose, 5 g glycerol, 5 g yeast extract, 5 g Hipolypepton, and 15 g agar per liter) containing 100 μg ml^{-1} kanamycin and 0.1% (vol/vol) acetic acid to eliminate *E. coli*. The transformants were inoculated on YPGD agar medium containing 30 μg ml^{-1} 5-fluorocytosine. 5-Fluorocytosine would be deaminated by the *codA* gene product cytosine deaminase to 5-fluorouracil that is toxic to *G. oxydans* cells due to the action of uracil phosphoribosyltransferase. The colonies that appeared were expected to have lost the *codA* gene via a homologous recombination. The recombinants were thus examined with respect to the size of the targeted genes. The candidate isolates showing expected PCR products were used as the gene deletion mutants (Kostner *et al*., 2013).

3.4.7 Preparation of the membranes

The cells were harvested in the late exponential growth phase by centrifugation at 9,000 × *g* for 10 min at 4°C and washed twice with 10 mM potassium phosphate (pH 7.0). The harvested cells were suspended at 1 g wet cells per 4 ml 10 mM potassium phosphate (pH 7.0), followed by addition of 0.5 mM phenylmethylsulfonyl fluoride. Then, the cell suspensions were passed twice through a French press (American Instrument Company, Silver Spring, MD) at 1,100 kg cm^{-2}. The eluents were centrifuged at 9,000 × *g* for 10 min at 4°C to remove the intact cells, and the supernatants were centrifuged again at 100,000 × *g* for 1 h at 4°C to precipitate the membranes. The precipitate was suspended with 10 mM potassium phosphate (pH 7.0), and the membranes were used for the experiments.

3.4.8 Analytical procedures

Protein concentrations were determined by the modified Lowry method with bovine serum albumin as the standard (Dulley and Grieve, 1975). Glucose, mannitol, and fructose were determined by means of a high-performance liquid chromatography (HPLC) system equipped with a refraction index (RI) detector as described previously (Kataoka *et al*., 2015). Acetic acid and 5-ketofructose were quantified using an ion exclusion column (RSpak KC-811, 8.0 mm [inside diameter] by 300 mm long; Shodex, Showa Denko KK, Kawasaki, Japan) at 60°C using 0.1% (wt/vol) phosphoric acid as the mobile phase at a flow rate of 0.4 ml min^{-1}. Acetic acid and 5-ketofructose were detected by RI and diode array detectors, respectively.

3.4.9 Enzyme assays

NDH activity was determined spectrophotometrically at 25°C by observing NAD(P)H oxidation at 340 nm. The reaction cocktail was composed of enzyme solution, 0.1 mM NAD(P)H, 50 mM potassium phosphate (pH 6.5), and 60 μM Q1. The millimolar extinction coefficients of NADH and NADPH were 6.3 and 6.2, respectively. One unit of enzyme activity was defined as the amount of enzyme oxidizing 1.0 μmol NAD(P)H per min.

Transhydrogenase (THase) activity in the membranes was measured spectrophotometrically using 3-acetylpyridine adenine dinucleotide (acetylpyridine-AD^+) at 25°C as described previously (Clarke and Bragg, 1985). In order to repress

the NADPH oxidation, the membranes were treated with 1% *n*-dodecyl-β-D-maltoside (DDM) for 1 h on ice prior to the enzyme assay. The reaction cocktail comprised an appropriate amount of DDM-treated membranes, 0.1 mM acetylpyridine-AD^+, 0.1 mM NADPH, and 50 mM potassium phosphate (pH 7.0). Reduction of acetylpyridine-AD^+ was monitored by absorbance at 375 nm. The millimolar extinction coefficient of acetylpyridine-ADH was 5.1. One unit of THase activity was defined as the amount of enzyme reducing 1.0 μmol acetylpyridine-AD^+ per min.

3.4.10 NAD(P)H/NAD(P)$^+$ measurements

The *G. oxydans* cells were cultivated on YPD medium and harvested in the mid-exponential growth phase. As the cell yields of the individual *G. oxydans* strains were different from one another, the cell density was normalized by OD_{600}. Intracellular levels of NAD(P)H and NAD(P)$^+$ were determined enzymatically using commercially available kits (BioAssay Systems, Hayward, CA), based on cyclic reduction of 3-(4,5-dimethylthiazolyl-2)-2,5-diphenyltetrazolium bromide (MTT) (Matsumura and Miyachi, 1980).

3.4.11 Data availability

The *G. oxydans* NBRC3293 genome sequence was deposited in DDBJ/EMBL/ GenBank under the accession numbers BARJ01000001 to BARJ01000024. The versions described here are the first versions.

Illumina sequence reads of NBRC3293 have been deposited in the DDBJ Sequence Read Archive (DRA) under accession number DRR041180. The BioProject identifier is PRJDB1087.

REFERENCES

Adachi O, Matsushita K, Shinagawa E, Ameyama M. 1979. Occurrence of old yellow enzyme in *Gluconobacter suboxydans*, and the cyclic regeneration of NADP. J Biochem 86:699–709. https://doi.org/10 .1093/oxfordjournals.jbchem.a132574.

Adachi O, Matsushita K, Shinagawa E, Ameyama M. 1980. Crystallization and characterization of NADP-dependent D-glucose dehydrogenase from *Gluconobacter suboxydans*. Agric Biol Chem 44:301–308. https://doi .org/10.1271/bbb1961.44.301.

Adachi O, Hours RA, Akakabe Y, Tanasupawat S, Yukphan P, Shinagawa E, Yakushi T, Matsushita K. 2010. Production of 4-keto-D-arabonate by oxidative fermentation with newly isolated *Gluconacetobacter liquefaciens*. Biosci Biotechnol Biochem 74:2555–2558. https://doi.org/10.1271/ bbb.100698.

Adachi O, Yakushi T. 2016. Membrane-bound dehydrogenases of acetic acid bacteria, p 273–297. *In* Matsushita K, Toyama H, Tonouchi N, Okamoto-Kainuma A (ed), Acetic acid bacteria: ecology and physiology. Springer Japan, Tokyo, Japan.

Altschul SF, Madden TL, Scha€ffer AA, Zhang J, Zhang Z et al. 1997. Gapped BLAST and PSI-BLAST: a new generation of protein database search programs. Nucleic Acids Res 25:3389–3402. https://doi .org/10.1093/nar/25.17.3389.

Ano Y, Hours RA, Akakabe Y, Kataoka N, Yakushi T, Matsushita K, Adachi O. 2017. Membrane-bound glycerol dehydrogenase catalyzes oxidation of D-pentonates to 4-keto-D-pentonates, D-fructose to 5-keto-D- fructose, and D-psicose to 5-keto-D-psicose. Biosci Biotechnol Biochem 81:411–418. https://doi.org/10.1080/09168451.2016.1254535.

Arai H, Sakurai K, Ishii M. 2016. Metabolic features of *Acetobacter aceti*. Acetic acid bacteria. Ecology and physiology. Springer. Japan.

Auriol C, Bestel-Corre G, Claude JB, Soucaille P, Meynial-Salles I. 2011. Stress-induced evolution of Escherichia coli points to original concepts in respiratory cofactor selectivity. Proc Natl Acad Sci 108:1278–1283.

Azuma Y, Hosoyama A, Matsutani M, Furuya N, Horikawa H, Harada T, Hirakawa H, Kuhara S, Matsushita K, Fujita N, Shirai M. 2009. Whole-genome analyses reveal genetic instability of *Acetobacter pasteurianus*. Nucleic Acids Res 37:5768–5783. https://doi.org/10.1093/nar/gkp612.

Boyer HW, Dussiox DR. 1969. A complementation analysis of restriction and modification of DNA in *Escherichia coli. J. Mol. Biol*, 41, 459-472. https://doi.org/10.1016/0022-2836(69)90288-5.

Brandt U. 2006. Energy converting NADH:quinone oxidoreductase (complex I). Annu Rev Biochem 75:69–92.

Bringer S, Bott M. 2016. Central Carbon Metabolism and Respiration in *Gluconobacter oxydans*. In: Matsushita K, Toyama H, Tonouchi N and Okamoto-Kainuma A (editors). Acetic Acid Bacteria. Tokyo: Springer. pp235–pp253.

Casadaban MJ. 1976. Transposition and fusion of the *lac* genes to selected promoters in *Escherichia coli* using bacteriophage lambda and Mu. J Mol Biol 104:541–555. https://doi.org/10.1016/0022-2836(76)90119-4.

Cava F, Zafra O, Magalon A, Blasco F, Berenguer J. 2004. A new type of NADH dehydrogenase specific for nitrate respiration in the extreme thermophile *Thermus thermophiles*. J Biol Chem 279: 45369-45378.

Clarke DM, Bragg PD. 1985. Cloning and expression of the transhydrogenase gene of *Escherichia coli*. J Bacteriol 162:367–373. https://doi.org/ 10.1128/JB.162.1.367-373.1985.

Delcher AL, Bratke KA, Powers EC, Salzberg SL. 2007. Identifying bacterial genes and endosymbiont DNA with Glimmer. Bioinformatics 23: 673–679. https://doi.org/10.1093/bioinformatics/btm009.

Deppenmeier U, Hoffmeister M, Prust C. 2002. Biochemistry and biotechnological applications of *Gluconobacter* strains. Appl Microbiol Biotechnol 60:233-242.

Desplats C, Beyly A, Cuine S, Bernard L, Cournac L, Peltier G. 2007. Modification of substrate specificity in single point mutants of *Agrobacterium tumefaciens* type II NADH dehydrogenase. FEBS Letters 581:4017-4022. https://doi.org/10.1016/j.febslet.2007.07.035.

Dulley JR, Grieve PA. 1975. A simple technique for eliminating interference by detergents in the Lowry method of protein determination. Anal Biochem 64:136–141. https://doi.org/10.1016/0003-2697(75)90415-7.

Elguindy MM, Nakamaru-Ogiso E. 2015. Apoptosis-inducing factor (AIF) and its family member protein, AMID, are rotenone-sensitive NADH: ubiquinone oxidoreductases (NDH-2). J Biol Chem 290:20815–20826. https://doi.org/10.1074/jbc.M115.641498.

Figurski DH, Helinski DR. 1979. Replication of an origin-containing derivative of plasmid RK2 dependent on a plasmid function provided in trans. Proc. Natl. Acad. Sci. U. S. A. 76:1648 –1652. https://doi.org/10.1073/ pnas.76.4.1648.

Gupta A, Singh VK, Qazi GN, Kumar A. 2001. *Gluconobacter oxydans*: its biotechnological applications. J. Mol. Microbiol. Biotechnol. 3(3):445-456.

Guy L, Kultima JR, Andersson SG. 2010. genoPlotR: comparative gene and genome visualization in R. Bioinformatics 26:2334–2335.

Hanahan D. 1983. Studies on transformation of *Escherichia coli* with plasmids. J Mol Biol 166:557–580. https://doi.org/10.1016/s0022 -2836(83)80284-8.

Hanke T, Richhardt J, Polen T, Sahm H, Bringer S, Bott M. 2012. Influence of oxygen limitation, absence of the cytochrome bc_1 complex and low pH on global

gene expression in *Gluconobacter oxydans* 621H using DNA microarray technology. J Biotechnol 157:359 –372. https://doi.org/10 .1016/j.jbiotec.2011.12.020.

Hanke T, Noh K, Noack S, Polen T, Bringer S, Sahm H, Wiechert W, Bott M. 2013. Combined fluxomics and transcriptomics analysis of glucose catabolism via a partially cyclic pentose phosphate pathway in *Gluconobacter oxydans* 621H. Appl Environ Microbiol 79:2336–2348. https://doi .org/10.1128/AEM.03414-12.

Heikal A, Nakatani Y, Dunn E, Weimar MR, Day CL, Baker EN, Lott JS, Sazanov LA, Cook GM. 2014. Structure of the bacterial type II NADH dehydrogenase: a monotopic membrane protein with an essential role in energy generation. Molecular Microbiology 91(5):950-964. https://doi.org/10 .1111/mmi.12507.

Kanchanarach W, Theeragool G, Inoue T, Yakushi T, Adachi O et al. 2010. Acetic acid fermentation of *Acetobacter pasteurianus*: relationship between acetic acid resistance and pellicle polysaccharide formation. Biosci Biotechnol Biochem 74:1591–1597.

Kanehisa M, Sato Y, Morishima K. 2016. BlastKOALA and GhostKOALA: KEGG tools for functional characterization of genome and metagenome sequences. J Mol Biol 428:726–731. https://doi.org/10.1016/j.jmb.2015 .11.006.

Kataoka N, Matsutani M, Yakushi T, Matsushita K. 2015. Efficient production of 2,5-diketo-D-gluconate via heterologous expression of 2-ketogluconate dehydrogenase in *Gluconobacter japonicas*. Appl Environ Microbiol 81:3552-3560. https://doi.org/10.1128/AEM.04176-14.

Kawai S, Goda-Tsutsumi M, Yakushi T, Kano K, Matsushita K. 2013. Heterologous overexpression and characterization of a flavoprotein-cytochrome *c* complex fructose dehydrogenase of *Gluconobacter japonicus* NBRC3260. Appl Environ Microbiol 79:1654 –1660. https://doi.org/10 .1128/AEM.03152-12.

Kerscher S, Drose S, Zickermann V, Brandt U. 2007. The three families of respiratory NADH dehydrogenases. Results Probl Cell Differ 45: 185-213. https://doi.org/10.1007/400_2007_028.

Kostner D, Peters B, Mientus M, Liebl W, Ehrenreich A. 2013. Importance of *codB* for new *codA*-based markerless gene deletion in *Gluconobacter* strains. Appl Microbiol Biotechnol 97:8341-8349. https://doi.org/10 .1007/s00253-013-5164-7.

Kostner D, Luchterhand B, Junker A, Volland S, Daniel R, Buchs J, Liebl W, Ehrenreich A. 2015. The consequence of an additional NADH dehydrogenase paralog on the growth of *Gluconobacter oxydans* DSM3504. Appl Microbiol Biotechnol 99:375-386. https://doi.org/10.1007/s00253-014 -6069-9.

Kovach ME, Elzer PH, Hill DS, Robertson GT, Farris MA, Roop RM, II, Peterson KM. 1995. Four new derivatives of the broad-host-range cloning vector pBBR1MCS, carrying different antibiotic-resistance cassettes. Gene 166:175–176. https://doi.org/10.1016/0378-1119(95)00584-1.

Krajewski V, Simic P, Mouncey NJ, Bringer S, Sahm, H, Bott M. 2010. Metabolic engineering of *Gluconobacter oxydans* for improved growth rate and growth yield on glucose by elimination of gluconate formation. Appl Environ Microbiol 76:4369-4376. https://doi.org/10 .1128/AEM.03022-09.

Kumar S, Stecher G, Tamura K. 2016. MEGA7: Molecular Evolutionary Genetics Analysis Version 7.0 for Bigger Datasets. Mol Biol Evol 33:1870–1874.

Macauley S, McNeil B, Harvey LM. 2001. The genus *gluconobacter* and its applications in biotechnology. Critical Reviews in Biotechnology 21(1):1-25.

Marmur J. 1961. A procedure for the isolation of deoxyribonucleic acid from micro-organisms. J Mol Biol 3:208–218, IN1. https://doi.org/10 .1016/S0022-2836(61)80047-8.

Marreiros BC, Sena FV, Sousa FM, Batista AP, Pereira MM. 2016. Type II NADH:quinone oxidoreductase family: phylogenetic distribution, structural diversity and evolutionary divergences. Environ Microbiol 18:4697–4709. https://doi.org/10.1111/1462-2920.13352.

Matsumura H, Miyachi S. 1980. Cycling assay for nicotinamide adenine dinucleotides. Methods Enzymol 69:465–470. https://doi.org/10.1016/ S0076-6879(80)69045-4.

Matsushita K, Ohnishi T, Kaback HR. 1987. NADH-ubiquinone oxidoreductases of the *Escherichia coli* aerobic respiratory chain. Biochemistry 26:7732–7737.

Matsushita K, Toyama H, Adachi O. 1994. Respiratory chains and bioenergetics of acetic acid bacteria. Advances in Microbial Physiology 36:247-301. https://doi.org/10.1016/s0065-2911(08)60181-2.

Matsushita K, Fujii Y, Ano Y, Toyama H, Shinjoh M, Tomiyama N, Miyazaki T, Sugisawa T, Hoshino T, Adachi O. 2003. 5-Keto-D-gluconate production is catalyzed by a quinoprotein glycerol dehydrogenase, major polyol dehydrogenase, in *Gluconobacter* species. Appl Environ Microbiol 69:1959–1966. https://doi.org/10.1128/aem.69.4.1959-1966.2003.

Matsutani M, Hirakawa H, Yakushi T, Matsushita K. 2011. Genome-wide phylogenetic analysis of *Gluconobacter, Acetobacter,* and *Gluconoacetobacter*. FEMS Microbiol let 315:122-128.

Matsutani M, Suzuki H, Yakushi T, Matsushita K. 2014. Draft genome sequence of *Gluconobacter thailandicus* NBRC 3257. Stand Genomic Sci 9:614–623. https://doi.org/10.4056/sigs.4778605.

Matsutani M, Ito K, Azuma Y, Ogino H, Shirai M et al. 2015. Adaptive mutation related to cellulose producibility in *Komagataeibacter medellinensis* (*Gluconacetobacter xylinus*) NBRC 3288. Appl Microbiol Biotechnol 99:7229–7240.

Matsutani M, Hirakawa H, Sriherfyna FH, Yakushi T, Matsushita K. 2019. Diversity of NADH dehydrogenases in acetic acid bacteria: adaptation to modify their phenotype through gene expansions and losses and neo- functionalization.

Microbiology (Reading) 165:287–291. https://doi.org/ 10.1099/mic.0.000774.

Mogi T, Matsushita K, Murase Y, Kawahara K, Miyoshi H, Ui H, Shiomi K, Omura S, Kita K. 2009. Identification of new inhibitors for alternative NADH dehydrogenase (NDH-II). FEMS Microbiol Lett 291: 157-161.

Mullins EA, Francois JA, Kappock TJ. 2008. A specialized citric acid cycle requiring succinyl-coenzyme A (CoA):acetate CoA-transferase (AarC) confers acetic acid resistance on the acidophile *Acetobacter aceti*. J Bacteriol 190:4933–4940.

Muynck CD, Pereira CSS, Naessens M, Parmentier S, Soetaert W, Vandamme EJ. 2007. The genus *Gluconobacter oxydans*: comprehensive overview of biochemistry and biotechnological applications. Critical reviews in biotechnology 27:147-171.

Nantapong N, Otofuji A, Migita CT, Adachi O, Toyama H, Matsushita K. 2005. Electron transfer ability from NADH to menaquinone and from NADPH to oxygen of type II NADH dehydrogenase of *Corynebacterium glutamicum*. Biosci. Biotechnol. Biochem 69: 149-159.

Neidhardt FC, Igraham JL, Schaechter M. 1990. Physiology of the bacterial cell. A molecular approach. Sinauer Associates, Inc. Massachusetts.

Peters JE, Thate TE, Craig NL. 2003. Definition of the *Escherichia coli* MC4100 genome by use of a DNA array. J Bacteriol 185:2017–2021. https://doi.org/10.1128/jb.185.6.2017-2021.2003.

Peters B, Junker A, Brauer K, Muhlthaler B, Kostner D, Mientus M, Liebl W, Ehrenreich A. 2013. Deletion of pyruvate decarboxylase by a new method for efficient markerless gene deletions in *Gluconobacter oxydans*. Appl Microbiol Biotechnol 97:2521–2530. https://doi.org/10 .1007/s00253-012-4354-z.

Prust C, Hoffmeister M, Liesegang H, Wiezer A, Fricke WF, Ehrenreich A, Gottschalk G, Deppenmeier U. 2005. Complete genome sequence of the acetic acid bacterium *Gluconobacter oxydans*. Nat Biotechnol 23: 195–200. https://doi.org/10.1038/nbt1062.

Richhardt J, Bringer S, Bott M. 2012. Mutational analysis of the pentose phosphate and Entner-Doudoroff pathways in *Gluconobacter oxydans* reveals improved growth of a Δ*edd* Δ*eda* mutant on mannitol. Appl Environ Microbiol 78:6975– 6986. https://doi.org/10.1128/AEM.01166-12.

Richhardt J, Bringer S, Bott M. 2013. Role of the pentose phosphate pathway and the Entner-Doudoroff pathway in glucose metabolism of *Gluconobacter oxydans* 621H. Appl Microbiol Biotechnol 97:4315–4323. https://doi.org/10.1007/s00253-013-4707-2.

Richter N, Neumann M, Liese A, Wohlgemuth R, Eggert T, Hummel W. 2009. Characterisation of a recombinant NADP-dependent glycerol dehydrogenase from *Gluconobacter oxydans* and its application in the production of L-glyceraldehyde.

Chembiochem 10:1888 –1896. https:// doi.org/10.1002/cbic.200900193.

Sainz F, Torija MJ, Matsutani M, Kataoka N, Yakushi T, Matsushita K, Mas A. 2016. Determination of dehydrogenase activities involved in D-glucose oxidation in *Gluconobacter* and *Acetobacter* strains. Frontiers in Microbiology 7: 1-14.

Sakamoto K, Miyoshi H, Matsushita K, Nakagawa M, Ikeda J, Ohshima M, Adachi O, Akagi T, Iwamura H. 1996. Comparison of the structural features of ubiquinone reduction sites between glucose dehydrogenase in *Escherichia coli* and bovine heart mitochondrial complex I. Eur J Biochem 237: 128 –135. https://doi.org/10.1111/j.1432-1033.1996.0128n.x.

Sakurai K, Arai H, Ishii M, Igarashi Y. 2011. Transcriptome response to different carbon sources in *Acetobacter aceti*. Microbiology 157:899–910.

Sakurai K, Arai H, Ishii M, Igarashi Y. 2012. Changes in the gene expression profile of *Acetobacter aceti* during growth on ethanol. J Biosci Bioeng 113:343–348.

Salichos L, Rokas A. 2013. Inferring ancient divergences requires genes with strong phylogenetic signals. Nature 497:327–331.

Salzberg SL, Delcher AL, Kasif S, White O. 1998. Microbial gene identification using interpolated Markov models. Nucleic Acids Res 26:544–548. https://doi.org/10.1093/nar/26.2.544.

Schafer A, Tauch A, Jager W, Kalinowski J, Thierbach G, Puhler A. 1994. Small mobilizable multi-purpose cloning vectors derived from the *Escherichia coli* plasmids pK18 and pK19: selection of defined deletions in the chromosome of *Corynebacterium glutamicum*. Gene 145:69–73. https:// doi.org/10.1016/0378-1119(94)90324-7.

Schweiger P, Gross H, Deppenmeier U. 2010. Characterization of two aldo-keto reductases from *Gluconobacter oxydans* 621H capable of regio- and stereoselective alpha-ketocarbonyl reduction. Appl Microbiol Biotechnol 87:1415–1426. https://doi.org/10.1007/s00253-010-2607-2.

Siedler S, Bringer S, Bott M. 2011. Increased NADPH availability in *Escherichia coli*: improvement of the product per glucose ratio in reductive whole-cell biotransformation. Appl Microbiol Biotechnol 92: 929 –937. https://doi.org/10.1007/s00253-011-3374-4.

Spero MA, Aylward FO, Currie CR, Donohue TJ. 2015. Phylogenomic analysis and predicted physiological role of the proton-translocating NADH:quinone oxidoreductase (complex I) across bacteria. MBio 6:6.

Spero MA, Brickner JR, Mollet JT, Pisithkul T, Amador-Noguez D et al. 2016. Different functions of phylogenetically distinct bacterial complex I Isozymes. J Bacteriol 198:1268–1280.

Stark MJ. 1987. Multicopy expression vectors carrying the *lac* repressor gene for

regulated high-level expression of genes in *Escherichia coli*. Gene 51:255–267. https://doi.org/10.1016/0378-1119(87)90314-3.

Sugisawa T, Hoshino T, Masuda S, Nomura S, Setoguchi Y, Tazoe M, Shinjoh M, Someha S, Fujiwara A. 1990. Microbial production of 2-keto-L-gulonic acid from L-sorbose and D-sorbitol by *Gluconobacter melanogenus*. Agric Biol Chem 54:1201–1209. https://doi.org/10.1271/bbb1961 .54.1201.

Suzuki H, Lefe□bure T, Bitar PP, Stanhope MJ. 2012. Comparative genomic analysis of the genus *Staphylococcus* including *Staphylococcus aureus* and its newly described sister species *Staphylococcus simiae*. BMC Genomics 13:38.

Tatusova T, Ciufo S, Fedorov B, O'Neill K, Tolstoy I. 2014. RefSeq microbial genomes database: new representation and annotation strategy. Nucleic Acids Res 42:D553–D559.

Yakushi T, Terada Y, Ozaki S, Kataoka N, Akakabe Y, Adachi O, Matsutani M, Matsushita K. 2018. Aldopentoses as new substrates for the membrane-bound, pyrroloquinoline quinone-dependent glycerol (polyol) dehydrogenase of *Gluconobacter* sp. Applied Microbiology and Biotechnology 102: 3159-3171. https://doi.org/10.1007/s00253-018-8848-1.

Yamada Y. 2016. Systematics of acetic acid bacteria. Acetic acid bacteria. Ecology and physiology. Springer. Japan.

Zerbino DR, Birney E. 2008. Velvet: algorithms for de novo short read assembly using de Bruijn graphs. Genome Res 18:821–829. https://doi .org/10.1101/gr.074492.107.

APPENDIX

Table S2.1. List of locus_tag numbers of *nuo* and *ndh* genes encoded in 53 AAB strains.

Strain	RefSeq ID	*nuoM*	Complex I_A (*nuoA-nuoN*)	Complex I_E (*nuoA-nuoN*)	*ndh (E)*	*ndh (Q)*
Acetobacter pasteurianus IFO 3191^T	GCA_000241625.1	APS_0276	APS_2240-APS_2228	-	APS_0805	APS_2095
Acetobacter pomorum DmCS_004	GCA_000755675.1	ApDm4_2573	ApDm4_1641-ApDm4_1653	-	ApDm4_2731	ApDm4_0193
Acetobacter fabarum KR	GCA_002276555.1	B8X00_02325	B8X00_04985-B8X00_05045	-	B8X00_03005	B8X00_11145
Acetobacter ghanensis LMG 23848^T	GCA_001499675.1	AGA_1241	AGA_2049-AGA_1241	-	AGA_1098	AGA_655
Acetobacter syzygii 9H-2^T	GCA_000964225.1	Absy_009_040	Absy_003_036-Absy_003_024	-	Absy_009_176	Absy_027_085
Acetobacter indonesiensis 5H-1^T	GCA_000963945.1	Abin_015_034	Abin_007_038-Abin_007_026	-	Abin_006_121	-
Acetobacter tropicalis NBRC16470^T	GCA_000787635.2	ATR1_067d0194	ATR1_072d0038-ATR1_072d0026	ATR1_453c0035-ATR1_453c0047	ATR1_075d0119	-
Acetobacter cibinongensis 4H-1^T	GCA_000963925.1	Abci_010_120	Abci_016_123-Abci_016_135	-	Abci_003_092	Abci_004_003
Acetobacter orientalis 21F-2^T	GCA_000963965.1	Abor_038_002	Abor_006_171-Abor_006_183	-	Abor_001_074	Abor_038_002
Acetobacter orleanensis JCM 7639^T	GCA_000964205.1	Abol_014_068	Abol_010_024-Abol_010_036	-	Abol_021_117	-
Acetobacter cerevisiae LMG1625^T	GCA_001580535.1	AD928_11130	AD928_11750-AD928_11690	-	AD928_06355	AD928_01565
Acetobacter malorum LMG 1746^T	GCA_001580615.1	AD930_02555	AD930_11890-AD930_11890	-	AD930_04005	-
Acetobacter aceti NBRC 14818^T	GCA_000963905.1	Abac_058_030	Abac_009_089-Abac_009_101	Abac_053_015-Abac_053_003	Abac_006_159	-
Acetobacter nitrogenifigens LMG 23498^T	GCA_000429165.1	G442_RS0103510	G442_RS0107345-G442_RS0107285	-	G442_RS0115185	-
Acetobacter persici DmL_053	GCA_002153675.1	HK19_05720	HK19_10985-HK19_11045	-	HK19_02685	-
Acetobacter okinawensis DsW_060	GCA_002153655.1	HK26_11985	HK26_00110-HK26_00050	-	HK26_07905	HK26_13250
Acetobacter senegalensis LMG23690^T	GCA_001580995.1	AD948_03670	AD948_11420-AD948_11480	AD948_16235-AD948_16175	AD948_13065	AD948_14735
Komagataeibacter nataicola RZS01	GCA_002009295.1	B0W47_06720	B0W47_04085-B0W47_04025	-	B0W47_00335, B0W47_00385	-
Komagataeibacter xylinus NBRC 15237^T	GCA_001571345.1	GXY01S_RS06595	GXY01S_RS04200-GXY01S_RS04260	-	GXY01S_RS03040, GXY01S_RS03090	-
Komagataeibacter rhaeticus AF1	GCA_000700985.1	GLUCORHAEAF1_17185	GLUCORHAEAF1_05835-GLUCORHAEAF1_05775	-	GLUCORHAEAF1_02515, GLUCORHAEAF1_19210	-
Komagataeibacter medellinensis NBRC 3288^T	GCA_000182745.2	GLX_12600	GLX_08770-GLX_08650	-	GLX_02910, GLX_11740	-
Komagataeibacter intermedius TF2^T	GCA_000964425.1	Gain_0050_028	Gain_0026_001-Gain_0026_013	Gain_0027_093-Gain_0027_105	Gain_0013_010, Gain_0013_019	-
Komagataeibacter oboediens 174Bp2	GCA_000227565.1	GOB01_RS09620	GOB01_RS00745-GOB01_RS00805	-	GOB01_RS12250, GOB01_RS15150, GOB01_RS15195	-
Komagataeibacter europaeus LMG 18890^T	GCA_000285295.1	GEU01_RS03665	GEU01_RS07445-GEU01_RS07415, GEU01_RS22700-GEU01_RS12165	GEU01_RS11020-GEU01_RS11080	GEU01_RS10370, GEU01_RS15555	-
Komagataeibacter hansenii JCM 7643^T	GCA_000964405.1	Gaha_0346_017	Gaha_0136_019-Gaha_0136_007	-	Gaha_0029_008, Gaha_0183_014	-
Gluconacetobacter diazotrophicus PAl 5^T	GCA_000021325.1	Gdia_1407	Gdia_3328-Gdia_3340	Gdia_0718-Gdia_0706	Gdia_2371	-
Tanticharoenia sakaeratensis NBRC 103193^T	GCA_000963885.1	-	-	Tasa_010_088-Tasa_010_076	Tasa_004_138	-
Asaia bogorensis NBRC 16594^T	GCA_001547995.1	-	-	Asbog_02417-Asbog_02405	Asbog_01958	-
Asaia platycodi SF2.1	GCA_000724025.1	-	-	ASAP_2930-ASAP_2942	ASAP_0407	-
Kozakia baliensis DSM 14400^T	GCA_001787335.1	-	-	A0U89_00960-A0U89_01020	A0U89_02980	-
Neoasaia chiangmaiensis NBRC 101099^T	GCA_002005465.1	-	-	A0U93_12845-A0U93_12905	A0U93_05005, A0U93_06520	-
Acidomonas methanolica NBRC 104435^T	GCA_000617865.1	-	-	Amme_027_018-Amme_027_029	Amme_085_055	-
Saccharibacter floricola DSM 15669^T	GCA_000378165.1	-	-	-	F457_RS0109250	-
Parasaccharibacter apium g773c	GCA_002079945.1	-	-	-	B6V90_RS05300	-
Bombella intestini R-52487^T	GCA_002003665.1	-	-	-	AL01_05990	-
Neokomagataea thailandica NBRC 106555^T	GCA_000378165.1	-	-	-	NTH01S_RS05025	NTH01S_RS02130
Gluconobacter roseus LMG 1418^T	GCA_001580885.1	-	-	-	AD943_01745	-
Gluconobacter oxydans 621H	GCA_000011685.1	-	-	-	GOX1675	-
Gluconobacter oxydans DSM 3504	GCA_000583855.1	-	-	-	GLS_c17910	GLS_c05650
Gluconobacter albidus NBRC 3250^T	GCA_002723915.1	-	-	-	GAL01_RS02200	GAL01_RS03755
Gluconobacter frateurii NBRC 3264^T	GCA_002723955.1	-	-	-	GFR01_RS01630	GFR01_RS09320, GFR01_RS10240
Gluconobacter thailandicus F149-1 = NBRC 10(	GCA_000964465.1	-	-	Gbth_003_046-Gbth_003_034	Gbth_024_155	Gbth_047_044
Gluconobacter japonicus NBRC 3271^T	GCA_002723975.1	-	-	-	GJA01_RS00785	GJA01_RS04680
Gluconobacter cerinus CECT 9110	GCA_001645165.1	-	-	-	A0123_00936	A0123_01576
Gluconobacter morbifer G707^T	GCA_000234355.1	-	-	-	GMO_03660	GMO_25120
Commensalibacter intestini A911^T	GCA_000231445.1	CIN_03320	CIN_06670-CIN_06790	-	-	CIN_16440
Granulibacter bethesdensis CGDNIH1^T	GCA_000231445.1	GbCGDNIH1_0708	GbCGDNIH1_1302-GbCGDNIH1_1289	-	GbCGDNIH1_1652	-
Acidiphilium angustum ATCC 35903^T	GCA_000701585.1	-	T342_RS0104625-T342_RS0104555	T342_RS0105795-T342_RS0105855	-	-
Acidiphilium cryptum JF-5	GCA_000016725.1	-	Acry_0921-Acry_0934	Acry_1120-Acry_1108	-	-
Acidiphilium multivorum AIU301^T	GCA_000202835.1	-	ACMV_09660-ACMV_09530	ACMV_07750-ACMV_07870	-	-
Acidiphilium rubrum ATCC 35905^T	GCA_900156265.1	-	SAMN05421828_106138-SAMN05421828_106152	SAMN05421828_101104-SAMN05421828_10192	-	-
Acidocella aminolytica 101 = DSM 11237^T	GCA_000964385.1	-	Aam_026_032-Aam_026_019	-	Aam_045_021	-
Acidocella facilis ATCC 35904^T	GCA_000687875.1	-	T331_RS0108740-T331_RS0108675	-		-

Table S2.3. List of missing or additional *nuo* and *ndh* genes encoded in no reference AAB strains. Gene repertoire between reference strain and target strain, which belongs to same species, was compared each other. If target strain have different gene repertoire, differences are shown in Table.

Strain	RefSeq ID	Distribution of additional / missing genes	Complex I_E *(nuoA-nuoN)*	*ndh (E)*	*ndh (Q)*
Acetobacter aceti strain TMW2.1153	GCA_002005445.1	deletion of Complex I_E	-	-	-
Acetobacter malorum CECT 7742	GCA_001642635.1	additional *ndh (Q)*	-	-	Amal_03563
Acetobacter malorum DmCS_005	GCA_000743885.1	additional *ndh (E)*	-	AmDm5_1578	-
Acetobacter orientalis DmW_048	GCA_002153685.1	deletion of *ndh (Q)*	-	-	-
Acetobacter pasteurianus subsp. ascendens SRCM101447	GCA_002173775.1	additional Complex I_E	S101447_01698-S101447_01684	-	-
Acetobacter pasteurianus subsp. paradoxus LMG 1591	GCA_001766255.1	deletion of *ndh (Q)*	-	-	-
Acetobacter pasteurianus subsp. pasteurianus SRCM101342	GCA_002173735.1	deletion of *ndh (Q)*	-	-	-
Acetobacter persici TMW2.1084	GCA_002006565.1	additional *ndh (Q)*, deletion of *ndh (E)*	-	-	A0U91_11370
Acetobacter tropicalis DmCS_006	GCA_000755665.1	additional *ndh (E)*	-	AtDm6_0233	-
Acetobacter tropicalis DmW_042	GCA_002153795.1	additional *ndh (E)*	-	HC62_11200	-
Acetobacter tropicalis NBRC 101654	GCA_000225485.1	additional *ndh (Q)*	-	-	ATPR_0997
Gluconobacter frateurii NBRC 101659	GCA_000284875.2	deletion of *ndh (E)*	-	-	-
Gluconobacter japonicus CECT 8443	GCA_001642615.1	additional *ndh (Q)*	-	-	A0J51_01291
Gluconobacter oxydans LMG 1399	GCA_001580635.1	deletion of *ndh (Q)*	-	-	-
Acetobacter aceti 1023	GCA_000691125.1	additional ndh (Q), deletion of Complex I_E	-	-	AZ09_09230
Gluconobacter oxydans 1.637	GCA_001680825.1	additional Complex I_E	BAR24_16480-BAR24_16540	-	-
Gluconobacter oxydans H24	GCA_000311765.1	additional Complex I_E	B932_1874-B932_1862	-	-
Gluconobacter oxydans WSH-003	GCA_000263255.1	additional Complex I_E	O1G_RS0110135-O1G_RS0110195	-	-
Gluconobacter frateurii M-2	GCA_000964445.1	deletion of *ndh (Q)*, additional Complex I_E	Gbfr_042_047-Gbfr_042_035	-	-
Komagataeibacter xylinus E25	GCA_000550765.1	additional Complex I_E	H845_1116-H845_1102	-	-
Komagataeibacter xylinus NBRC 13693	GCA_000964505.1	additional Complex I_E	Gxy13693_040_031-Gxy13693_040_019	-	-

Table S3.1. Summary characteristics for whole genome sequencing of *Gluconobacter oxydans* NBRC 3293 strain.

Assembly size (bp)	3,333,878
GC contents (%)	60.62
Total number of contigs:	24
Longest contig (bp):	577,752
N50 (bp)	340,045
L50	4
Estimated coverage (×)	240
CDS	3,141
rRNA genes	3
tRNA genes	51

BioProject accession number, PRJDB1087; DRA accession number, DRA003796; GenBank accession number, BARJ01000001-BARJ01000024.

Table S3.3. Genes involved in the metabolism on glucose, mannitol, and nicotinamide cofactors.

Gene	Enzyme	ATCC621H	DSM3504	NBRC3293
gdhM	GDH	GOX0265	GLS_c02870	NBRC3293_0040
sldA	GLDH (A)	GOX0854	GLS_c09380	NBRC3293_0818
sldB	GLDH (B)	GOX0855	GLS_c09390	NBRC3293_0819
gndS	GADH (S)	GOX1232	GLS_c13190	NBRC3293_1197
gndL	GADH (L)	GOX1231	GLS_c13180	NBRC3293_1196
gndC	GADH (C)	GOX1230	GLS_c13170	NBRC3293_1195
gno	5KGR	GOX2187	GLS_c23020	NBRC3293_2332
-	2KGR	GOX0417	GLS_c04360	NBRC3293_0196
gdhS	NADP-GDH	GOX2015	GLS_c21270	NBRC3293_2134
zwf	G6PDH	GOX0145	GLS_c01700	NBRC3293_2852
gnd	6PGDH	GOX1705	GLS_c18220	NBRC3293_1777
gapA	G3PDH	GOX0508	GLS_c06050	NBRC3293_0401
-	NADP-ALDH	GOX1122	GLS_c11910	NBRC3293_1095
-	Mannitol DH	GOX1432	GLS_c15490	NBRC3293_1450
kfr	KFR	GOX0859	GLS_c09430	NBRC3293_0824
pntA1	THase (A1)	GOX0310	GLS_c03310	NBRC3293_0090
pntA2	THase (A2)	GOX0311	GLS_c03320	NBRC3293_0091
pntB	THase (B)	GOX0312	GLS_c03330	NBRC3293_0092
ndhP	p-NDH	GOX1675	GLS_c17910	NBRC3293_1744
ndhA	a-NDH	-	GLS_c05650	NBRC3293_0375

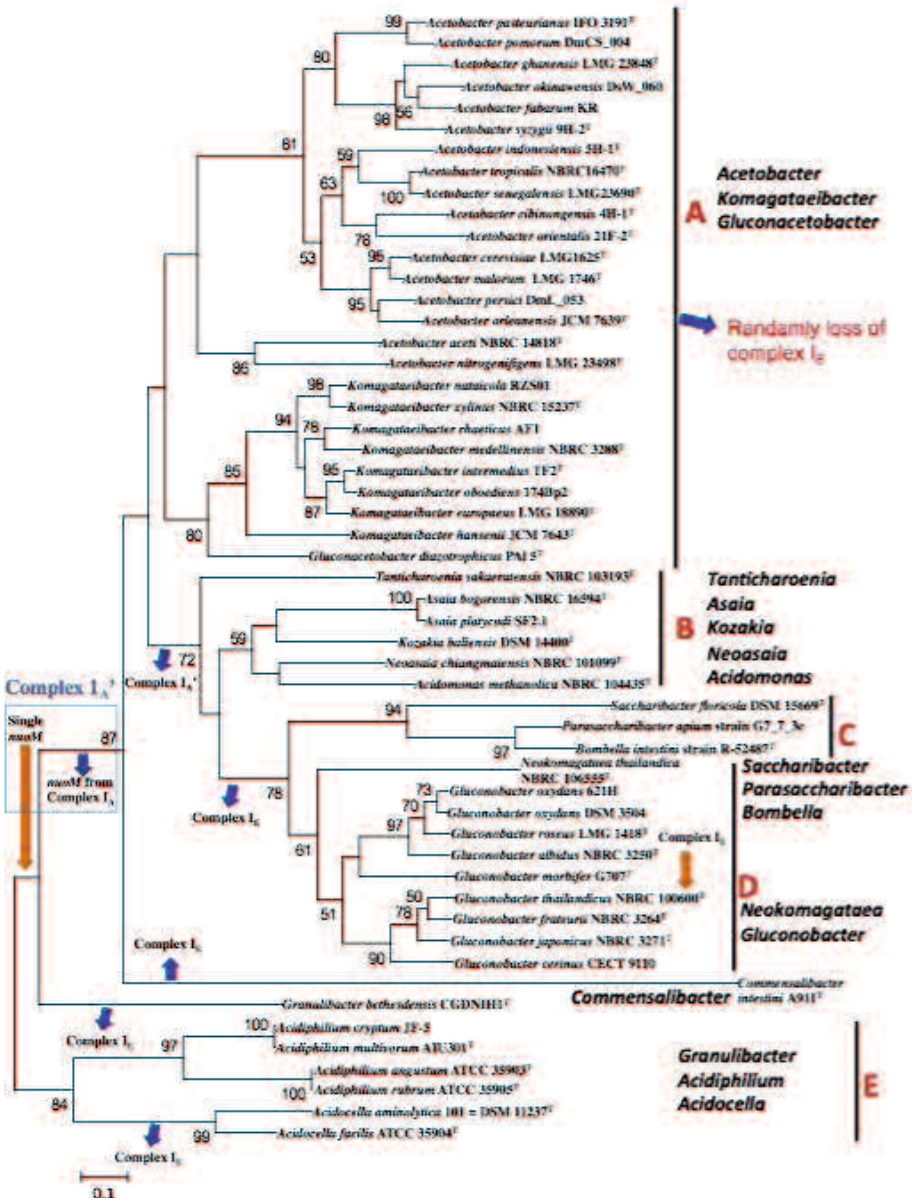

Fig. S2.1 Whole genome-based Maximum-likelihood phylogenetic trees of AAB strains using RAxML. Tree was prepared based on nucleotide sequences (352 orthologous gene set) of the genomes. In the genome-based tree, the gene-support frequency (GSF) is shown (Suzuki *et al*., 2012; Salichos and Rokas, 2013). Support frequency values above 50% were only shown. Orange and blue arrows indicate gene gain and loss, respectively. Complex I_A' is composed of Complex I_A operon without *nuoM* gene and single *nuoM* gene.

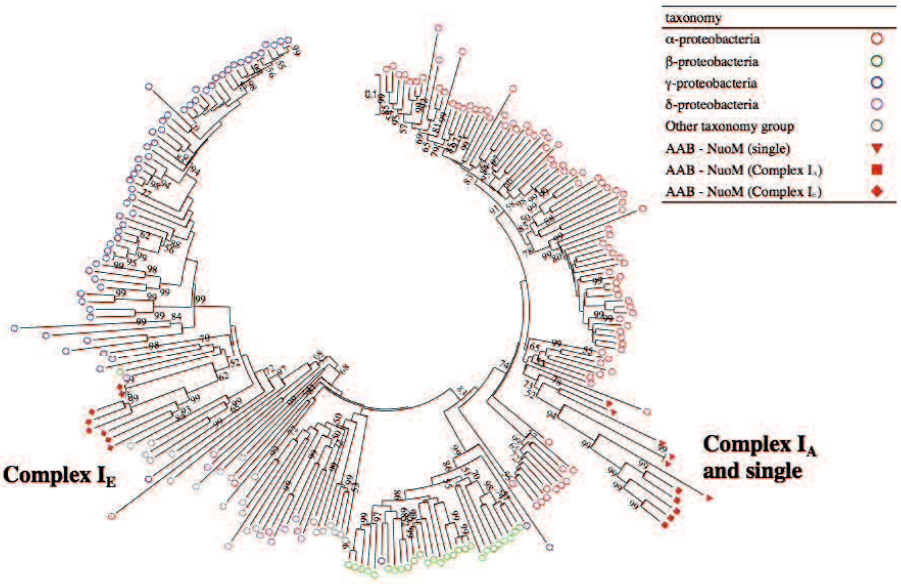

Fig. S2.2 An unrooted neighbour-joining phylogenetic tree of NuoM proteins in known bacterial genera. The phylogenetic tree was constructed using MEGA 7.01. The scale bar represents 0.1 substitutions per site.

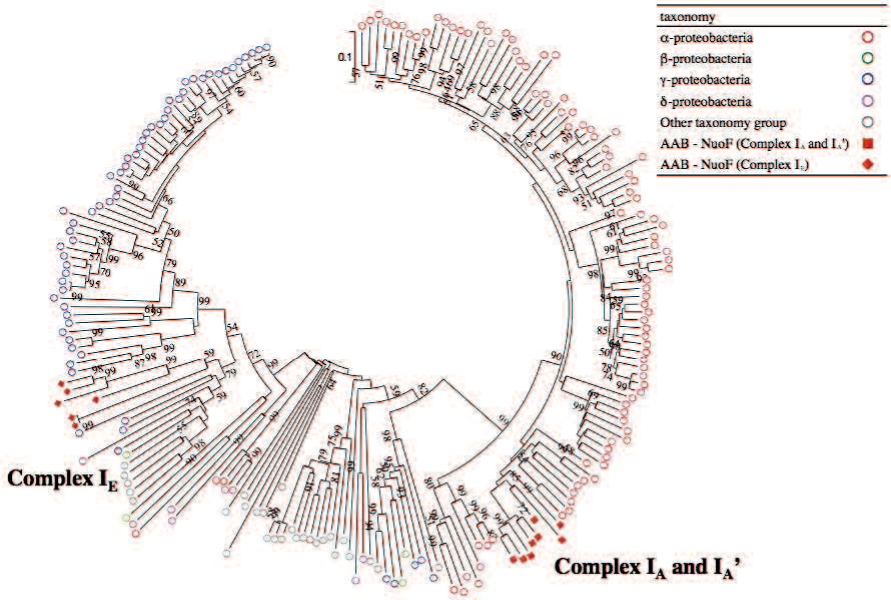

Fig. S2.3 An unrooted neighbour-joining phylogenetic tree of NuoF proteins in known bacterial genera. The phylogenetic tree was constructed using MEGA 7.01. The scale bar represents 0.1 substitutions per site.

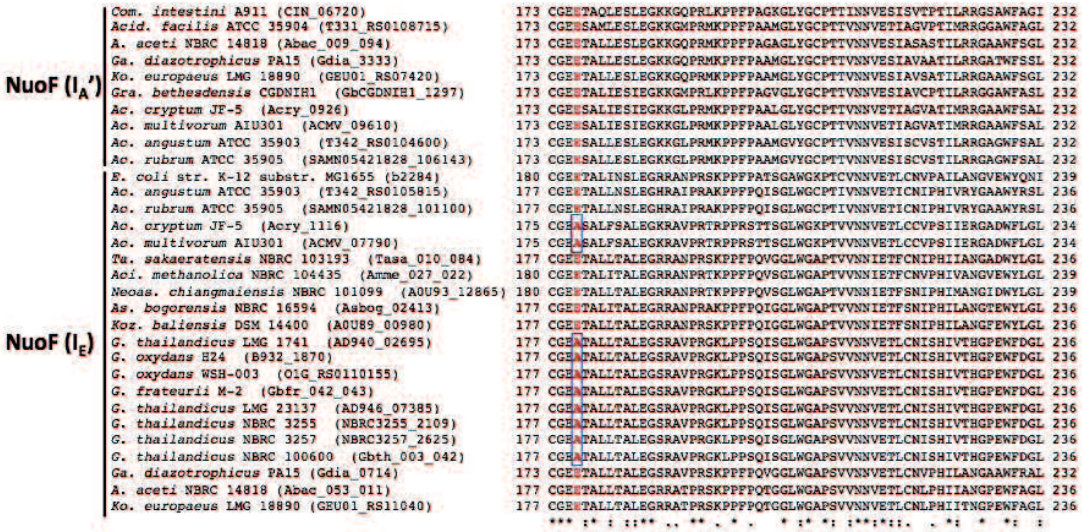

Fig. S2.4 Partial sequence alignment of the NuoF proteins of AAB. The bold red colour indicates the residues responsible for the NADPH-oxidizing ability.

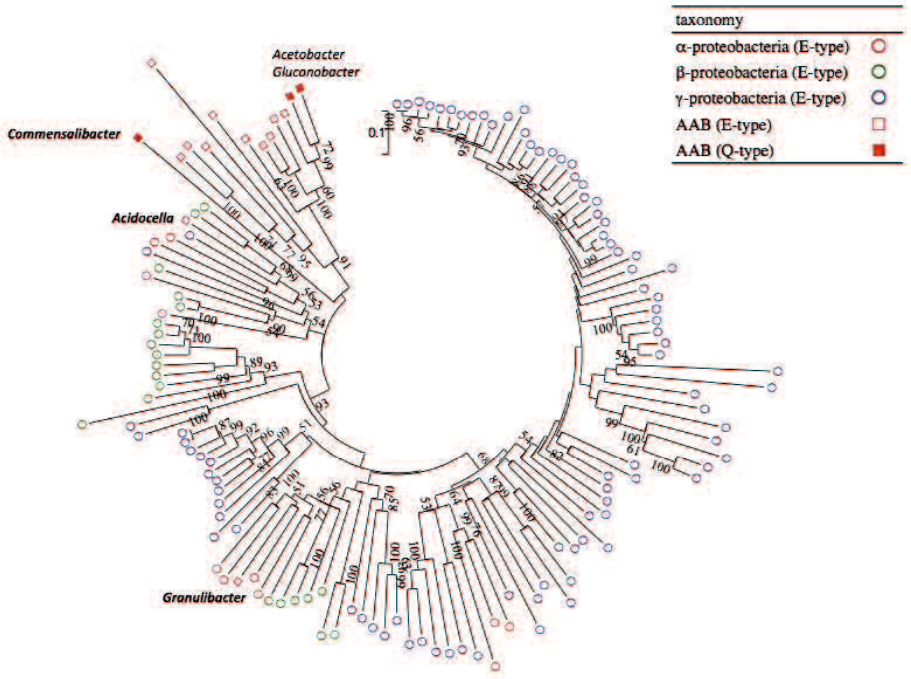

Fig. S2.5 An unrooted neighbour-joining phylogenetic tree of NdhII proteins in known bacterial genera. The phylogenetic tree was constructed using MEGA 7.01. The scale bar represents 0.1 substitutions per site.

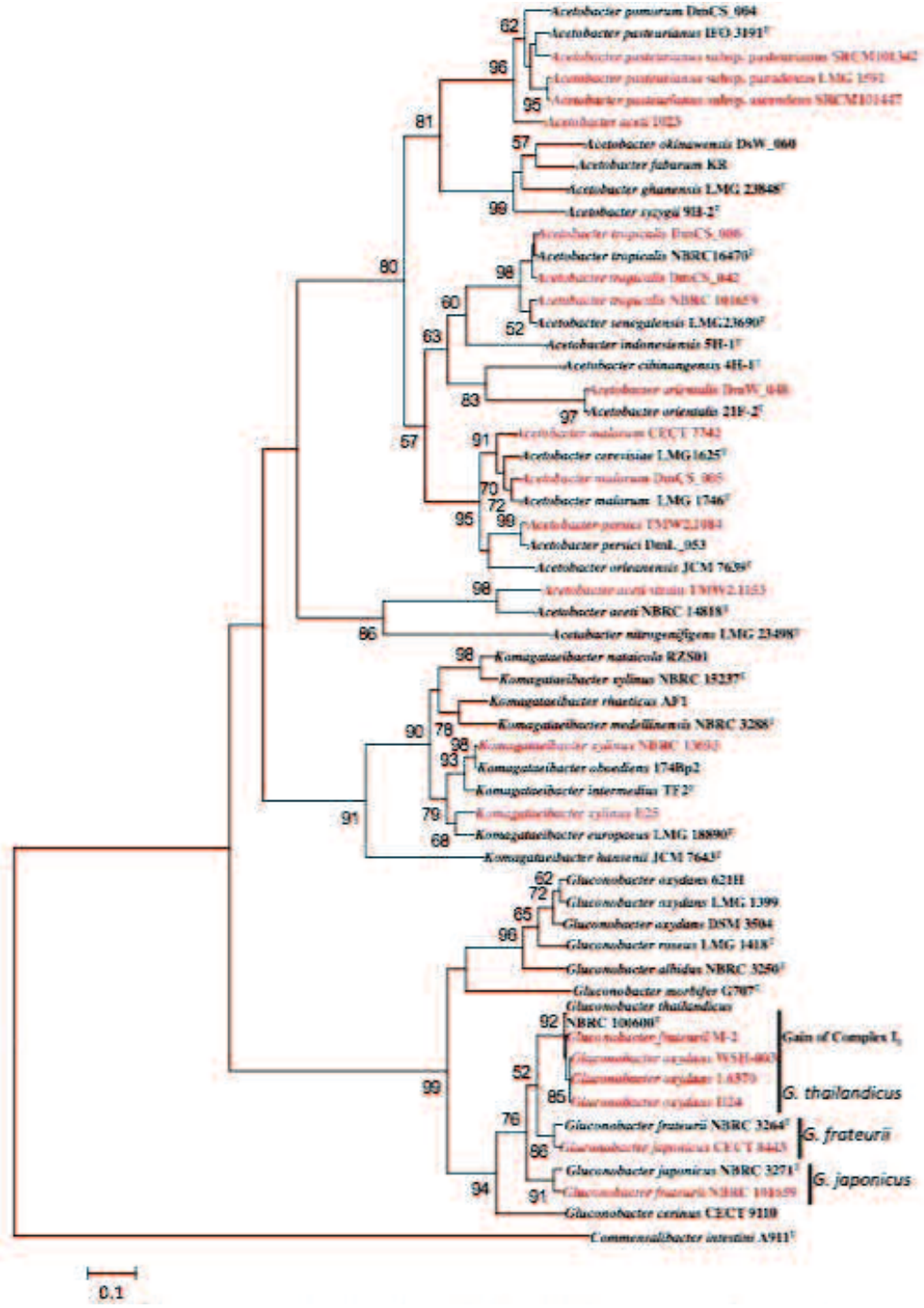

Fig. S2.6 Whole genome-based Maximum-likelihood phylogenetic trees of AAB strains using RAxML. Tree was prepared based on nucleotide sequences (364 orthologous gene set) of the genomes. In the genome-based tree, the gene-support frequency (GSF) is shown (Suzuki *et al*., 2012; Salichos and Rokas, 2013). Support frequency values above 50% were only shown. Red color indicates the strains shown in Table S2.3.

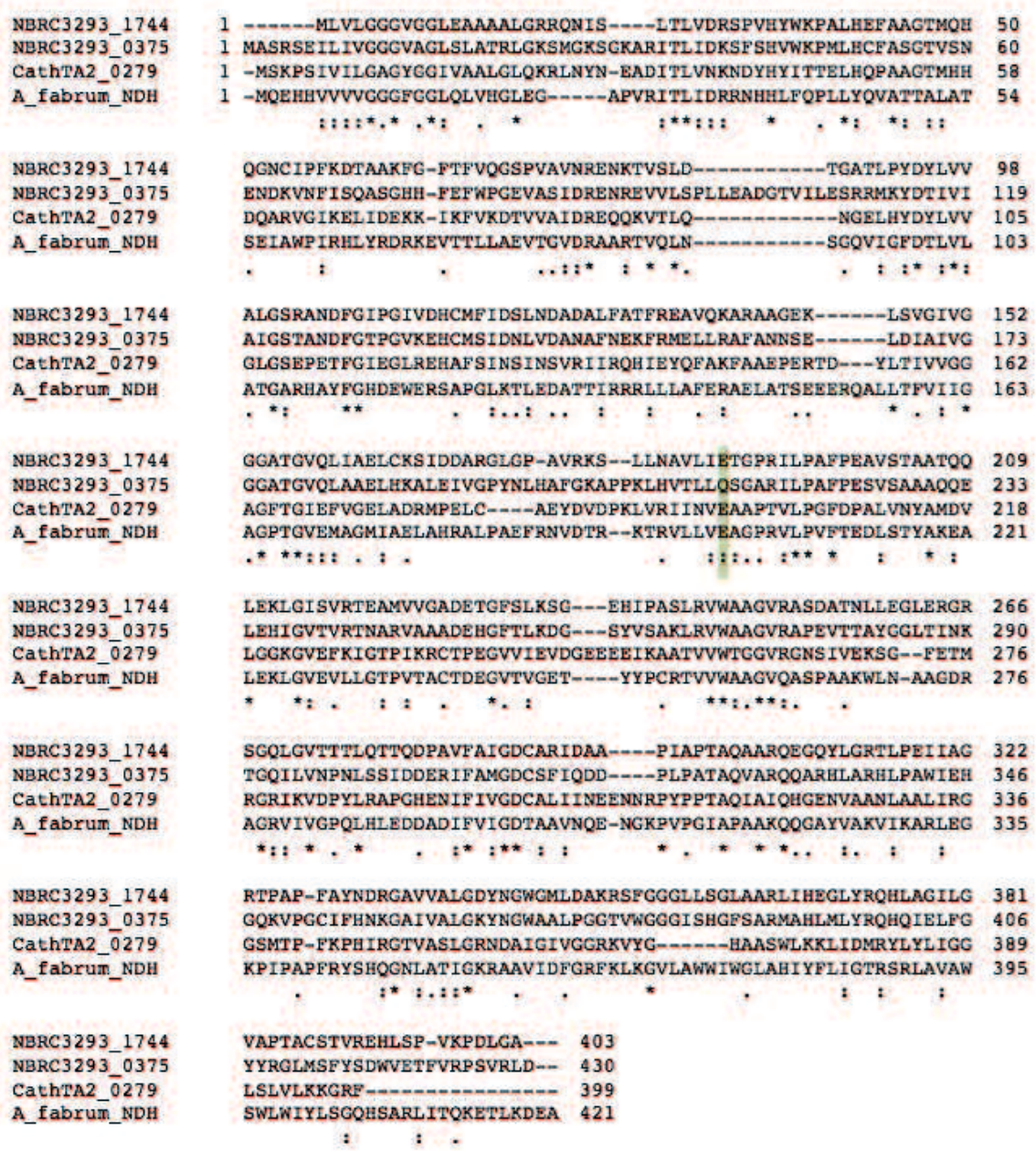

Fig. S3.1. An amino acid residue critical for substrate specificity in NDH. Amino acid sequence alignment of p-NDH (NBRC3293_1744), a-NDH (NBRC3293_0375), *Caldalkalibacillus thermarum* NDH (CathTA2_0279), and *Agrobacterium fabrum* NDH (A_fabrum_NDH) on ClustalX (ver. 2.0.12). The amino acid residue important for the substrate specificity is highlighted in green.

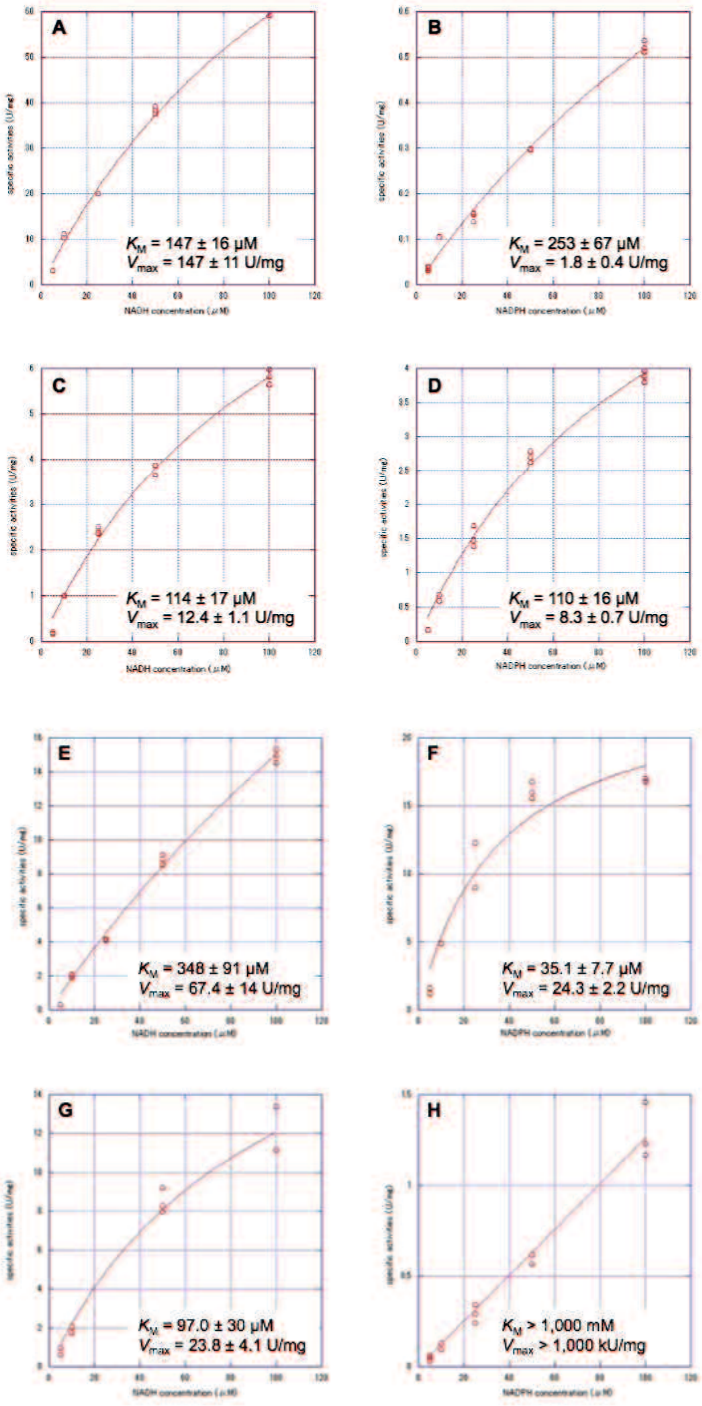

Fig. S3.2. Kinetic analysis for p-NDH (A and B), its E189Q derivative (C and D), a-NDH (E and F), and its Q213E derivative (G and H). The membranes of the recombinant *E. coli* strains that express *Gluconobacter* NDH as a sole NDH enzyme were used. NDH activity in the membranes was measured by examining the decrease in absorbance at 340 nm in the presence of 60 μM Q1. The K_M and V_{max} values were calculated on KaleidaGraph ver. 4.5 (Synergy Software, Reading, PA, USA).

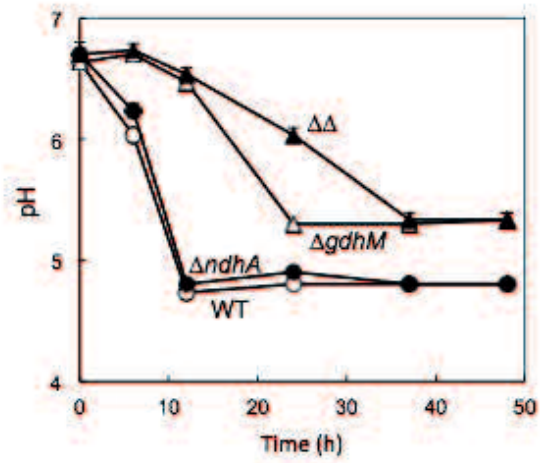

Fig. S3.3. Changes in pH of culture medium on the growth of the *G. oxydans* derivatives on glucose. The *G. oxydans* cells were cultivated as described in Fig. 3.3. The mean values and the standard deviations of triplicate cultivation are shown. White circle, wild type (WT); black circle, Δ*ndhA*; white triangle, Δ*gdhM*; black triangle, Δ*gdhM* Δ*ndhA* (ΔΔ).

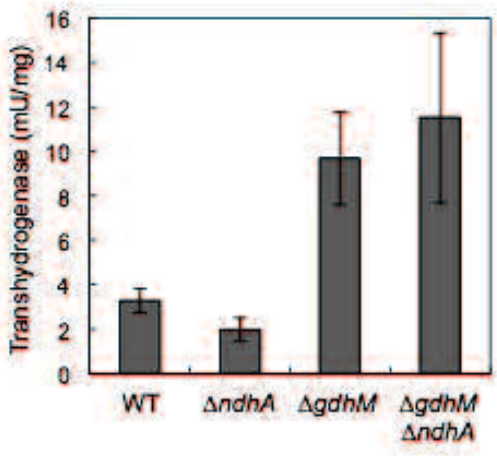

Fig. S3.4. Transhydrogenase activity in the membranes of *G. oxydans* derivatives grown on glucose. The *G. oxydans* cells were cultivated as described in Fig. 3.3, and harvested at the late-exponential growth phase. The membranes were treated with 1% n-dodecyl-β-D-maltoside prior to the enzyme assay. Transhydrogenase activity was measured with 3- acetylpyridine adenine dinucleotide and NADPH as described in the Materials and Methods section. The mean values and the standard deviations of triplicate enzyme assay are shown. WT, wild type.

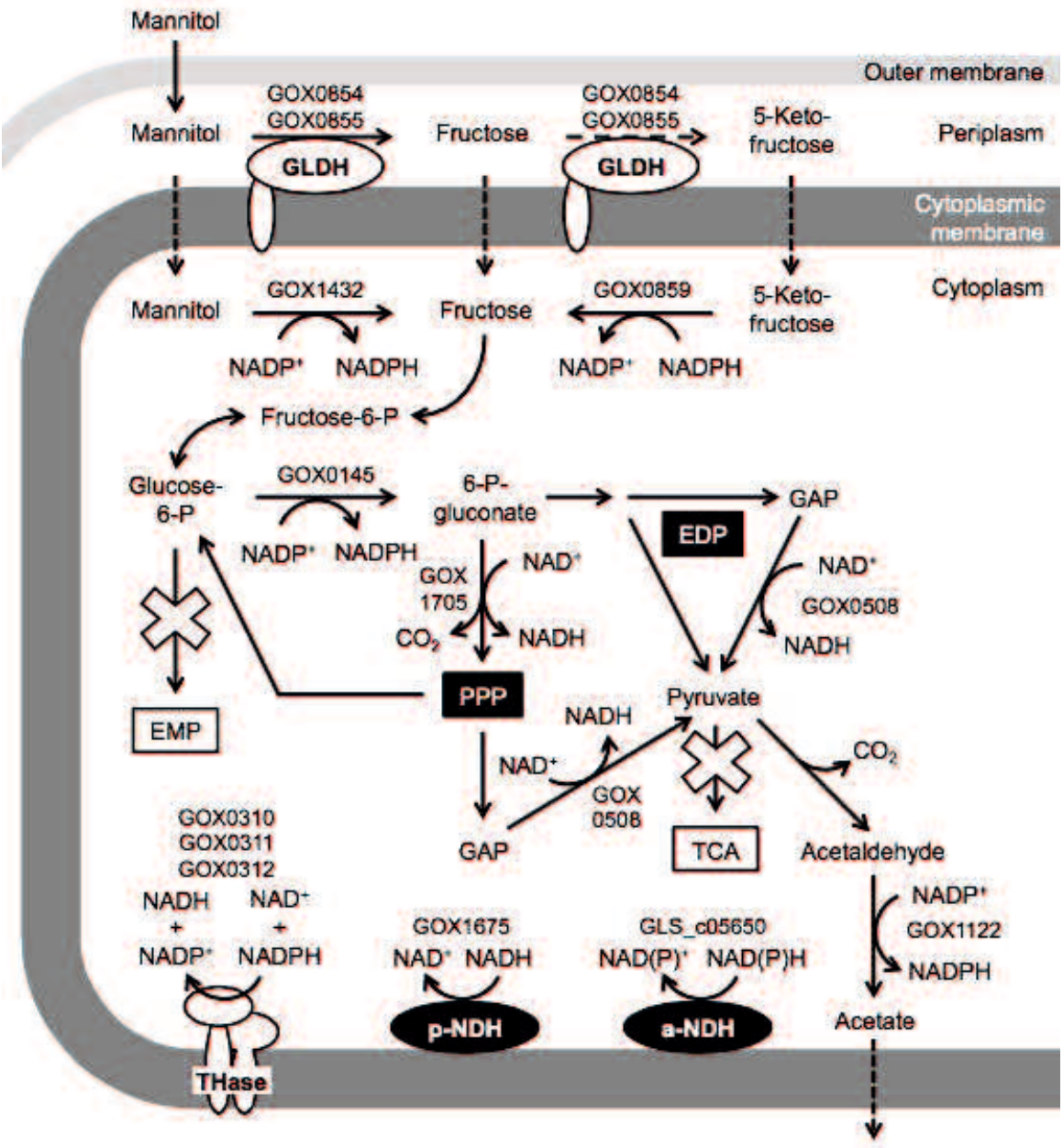

Fig. S3.5. Metabolism on mannitol and nicotinamide cofactors in *Gluconobacter oxydans* (Richhardt *et al*., 2012). Mannitol is metabolized into acetic acid via pentose phosphate pathway or Entner–Doudoroff pathway in *G. oxydans*. GLDH, membrane-bound glycerol dehydrogenase; EMP, Embden–Meyerhof–Parnas pathway; PPP, pentose phosphate pathway; EDP, Entner–Doudoroff pathway; TCA, tricarboxylic acid cycle; THase, transhydrogenase; p-NDH, primary NADH dehydrogenase; a-NDH, auxiliary NADH dehydrogenase.

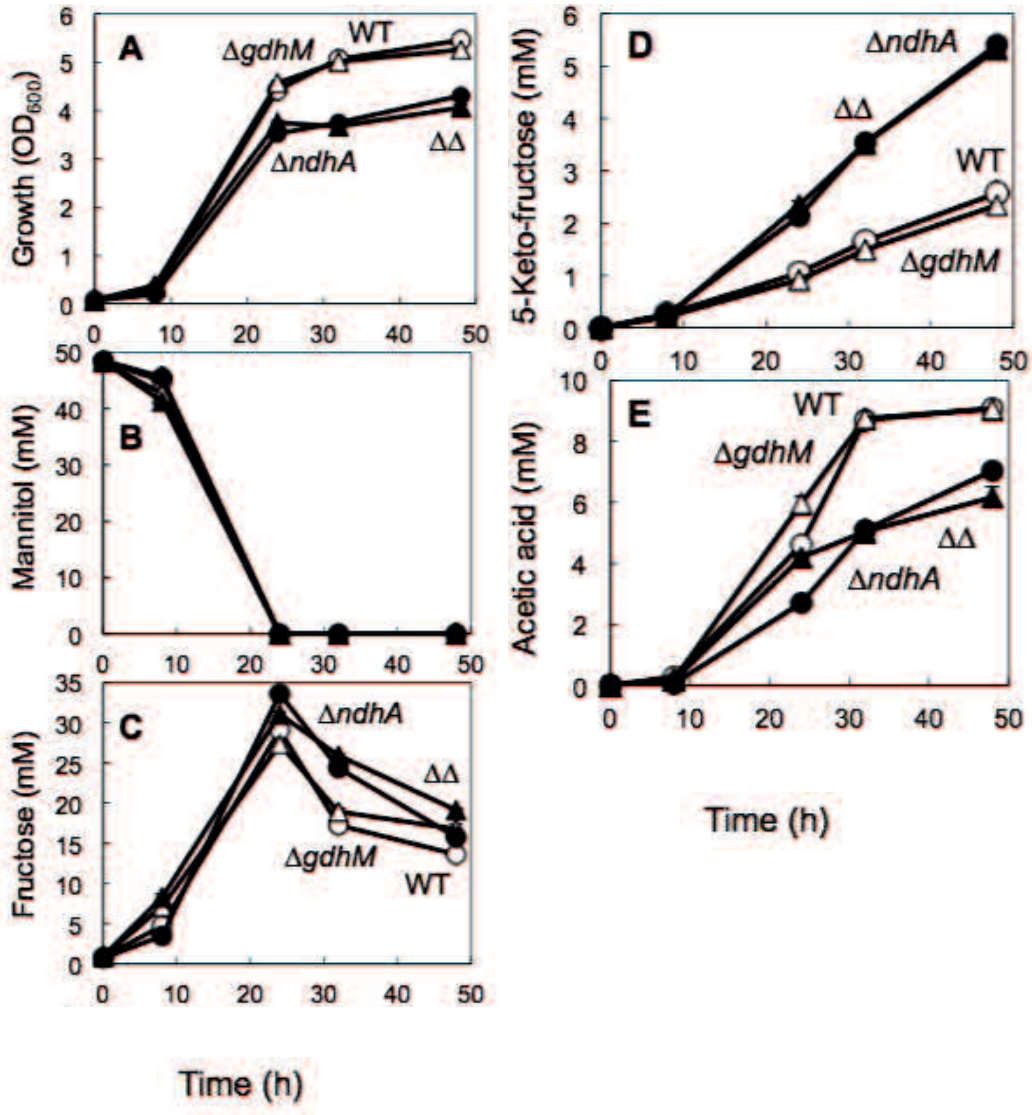

Fig. S3.6. Cultivation of the *G. oxydans* derivatives on mannitol. The *G. oxydans* cells were cultivated in mannitol medium under shaking at 200 rpm. The mean values of triplicate cultivation on OD_{600} for growth (A), mannitol (B), fructose (C), 5-ketofructose (D), and acetic acid (E) were plotted and the error bars represent the standard deviation. White circle, wild type (WT); white triangle, Δ*gdhM*; black circle, Δ*ndhA*; black triangle, Δ*gdhM* Δ*ndhA* (ΔΔ).

ACKNOWLEDGEMENTS

I would like to express my profound gratitude to my supervisor, Prof. Toshiharu Yakushi, for expert guidance, overwhelming support, indulgent, and encouragement to accomplish my study. I also would like to thank Prof. Kazunobu Matsushita, Asst. Prof. Dr. Naoya Kataoka, Dr. Minenosuke Matsutani, Prof. Osao Adachi, Prof. Mamoru Yamada, Assoc. Prof. Tomoyuki Kosaka for great support, accelerating discussion and valuable advice. I peculiarly thank to Nami Matsumoto, Shoko Emoto, Kensuke Hirano, Heru Nurcahyo, and all Obi members for their generous technical support and discussion.

I am grateful to Indonesian government (BUDI-LN scholarship) for their financial support, organized by the Ministry of Finance (Indonesian Endowment Fund for Education/LPDP) and the Ministry of Research, Technology and Higher Education, MEXT KAKENHI, Japan Society for the Promotion of Science and Brawijaya University, Indonesia.

I also would like to express my sincere gratitude to my mother and my brother (Pras), my husband (Mochamad Nurcholis), and my son (Fychoyama) for their wholehearted support, sacrifice, understanding, and encouragement.

Feronika Heppy Sriherfyna

PhD Student of Graduate School of
Sciences and Technology for Innovation
Yamaguchi University

SUMMARY

The Diversity and Physiological Roles of NADH Dehydrogenase in Acetic Acid Bacteria

NADH dehydrogenase, an enzyme catalyzing electron transfer from NAD(P)H to ubiquinone subsequently oxygen as a terminal electron acceptor, is one of pivotal enzymes undertaking respiration process in the central metabolism system and supporting the growth of microorganism, including acetic acid bacteria (AAB). NADH dehydrogenase is divided into four types, including type I NADH dehydrogenase (Complex I or NDH-1), type II or alternative NADH dehydrogenase (NDH-2), sodium pumping NADH dehydrogenase (Nqr), and type IV NADH dehydrogenase involving in nitrate respiration in the *Thermus thermophiles*, an extreme thermophilic bacterium. The type I and type II NADH dehydrogenases are encoded in the *nuo* and *ndh* genes, respectively. The type I and type II NADH dehydrogenases possessed by AAB were studied and this study revealed that these gene distributions were in accordance with the phylogenetic relationships. This study revealed that the type I comprised complex I_A and complex I_E, where *nuoC* and *nuoD* are fused as *nuoC/D* in the complex I_E gene cluster. The additional type of type I NADH dehydrogenase belonging to genera *Acetobacter*, *Gluconobacter*, and *Komagataeibacter* is complex I_A' which lacks the *nuoM* gene from the complex I_A gene cluster. In case of type II NADH dehydrogenase, NDH, nearly all AAB rule out of early-diverged species bearing *ndh* gene, whereas the amino acid residue replacement in *ndh* gene directing the capability in oxidizing NADPH is owned by some species.

Gluconobacter oxydans NBRC3293, a gram negative and obligate aerobe bacterium belong to *Acetobacteraceae* family, possesses two NDHs, primary NDH (p-NDH) and auxiliary NDH (a-NDH) oxidizing NAD(P)H generated from pentose phosphate pathway and Entner-Doudoroff pathway due to lack of phosphofructokinase and succinate dehydrogenase in Embdem-Myerehof-Parnas pathway and TCA cycle. These bacteria utilize sugar or sugar alcohol as a carbon source and have two metabolic systems consist of nicotinamide independent-periplasmic and nicotinamide cofactor dependent-cytoplasmic oxidation systems.

Several enzymes perform in the central metabolism system comprising membrane-bound glucose dehydrogenase (GdhM) and glycerol dehydrogenase (GLDH) oxidizing glucose into gluconic acid and 5-ketogluconic acid in the periplasm, respectively. GdhM deficiency leads to uptake most of glucose into cytoplasm and assumed to affect the intracellular redox balance. To characterize biochemical properties of the two NDHs, heterologous expression in *E. coli* DKO strain devoid of type I and type II NADH dehydrogenase was conducted. It is revealed that p-NDH has a specificity to NADH, whilst a-NDH oxidizes both NADH and NADPH. Therefore, this study suggests that a-NDH play a role in NADPH oxidation of *G. oxydans*. To elucidate the physiological role of a-NDH, *G. oxydans* NBRC3293 derivatives defective of a-NDH were constructed. Elimination of *ndhA* gene showed similar growth rate to wild-type strain in glucose medium, whereas under the Δ*gdhM* background, the mutant showed less growth compare to its parental strain. The intracellular redox investigation performed elevated NADPH level in the double mutant strain that becomes a plausible reason of its limiting cell growth. Due to periplasmic oxidation system blocked, the cell utilized cytoplasmic oxidation system that relies on the presence of a-NDH to release a "metabolic jam". A similar phenomenon also took place when *G. oxydans* NBRC3293 cultivated in mannitol medium.

LIST OF PUBLICATIONS

1. **Diversity of NADH dehydrogenase in acetic acid bacteria: adaptation to modify their phenotype through gene expansions and losses and neo-functionalization**

   Minnenosuke Matsutani, Hideki Hirakawa, Feronika Heppy Sriherfyna, Toshiharu Yakushi, and Kazunobu Matsushita

   Microbiology, 2019, 165:287-291. DOI: 10.1099/mic.0.000774.

2. **The auxiliary NADH dehydrogenase plays a crucial role in redox homeostasis of nicotinamide cofactors in the absence of the periplasmic oxidation system in *Gluconobacter oxydans* NBRC3293**

   Feronika Heppy Sriherfyna, Minnenosuke Matsutani, Kensuke Hirano, Hisashi Koike, Naoya Kataoka, Tetsuo Yamashita, Eiko Nakamura-Ogiso, Kazunobu Matsushita, Toshiharu Yakushi

   Applied and Environmental Microbiology, 2021, Volume 87:02155-20. DOI: 10.1128/AEM.02155-20.

BIOGRAPHY

Name : Feronika Heppy Sriherfyna
Date of birth : October 18th, 1983
Place of birth : Malang, East Java, Indonesia

Institute Attended

1. Department of Agroindustrial Product Technology, Brawijaya University, Indonesia (2002-2007): B.Sc. of Food Science
2. Department of Agroindustrial Biotechnology, Brawijaya University, Indonesia (2007-2010): M.Sc. of Biotechnology
3. Applied Microbiology, Graduate School of Science and Technology for Innovation, Yamaguchi University, Japan (2016-2021): PhD of Life Science

Scholarship

1. Double degree program, BU-DIKNAS Scholarship, Ministry of Education and Culture (2007-2010)
2. BUDI-LN scholarship, Ministry of Finance (Indonesian Endowment Fund for Education/LPDP) and Ministry of Research, Technology and Higher Education (2016-2020).

Presentation

1. The 12th Young Scientist Seminar, Aio, Yamaguchi, Japan. Title: Optimization production, purification and partial characterization of fructosyltransferase (FTase) from *Aspergillus* sp. WN1C.
2. The 13th Young Scientist Seminar, Aio, Yamaguchi, Japan. Title: Biochemical characterization of type II NADH dehydrogenase of *Gluconobacter oxydans* NBRC3293.
3. Yamaguchi University Annual Microbiology Meeting 2017. Title: Studies on physiological role of two type II NADH dehydrogenase in *Gluconobacter* sp.
4. The 91st Annual Meeting of the Japanese Biochemical Society 2018, Kyoto, Japan Title: Characterization of two species of type II NADH dehydrogenases in *Gluconobacter* sp.

5. The 15th Young Scientist Seminar, Aio, Yamaguchi, Japan. Title: Function of two type II NADH dehydrogenase of *Gluconobacter oxydans* NBRC3293.
6. Yamaguchi University Annual Microbiology Meeting 2018. Title: Identification of two species of type II NADH dehydrogenases in *Gluconobacter* sp.
7. The 53rd Meeting of the Chu-Shikoku Branch of the Japanese Society of Agricultural Chemistry 2019, Kochi, Japan. Title: Biochemical and physiological properties of type II NADH dehydrogenases of *Gluconobacter oxydans* NBRC3293.
8. The 60th Annual Meeting of the Chushi Branch of the Japanese Biochemical Society 2019, Ube, Yamaguchi, Japan. Title: Role of type II NADH dehydrogenase in *Gluconobacter* species, a member of acetic acid bacteria.
9. The 54th Meeting of the Chu-Shikoku Branch of the Japanese Society of Agricultural Chemistry 2019, Okayama, Japan. Title: Glucose metabolism in the *Gluconobacter* mutant strain that lost the glucose-oxidation ability.
10. The 16th Young Scientist Seminar, Aio, Yamaguchi, Japan. Title: NADH and NADPH oxidation in the mutant strain of *Gluconobacter oxydans* NBRC3293 lost the membrane-bound glucose dehydrogenase grown on glucose.
11. The 17th Young Scientist Seminar, Yamaguchi, Japan. Title: The effect of auxiliary NADH dehydrogenase deficiency in intracellular NAD(P)H/NAD(P)$^+$ level of *Gluconobacter oxydans* NBRC3293.